Thesis for the degree of Doctor of Philosophy

The Balanced Electromagnetic Separation Transducer for Bone Conduction Audiometry and Hearing Rehabilitation

by

Karl-Johan Fredén Jansson

Department of Electrical Engineering
Biomedical Signals and Systems Group
CHALMERS UNIVERSITY OF TECHNOLOGY

Göteborg, Sweden 2017

The Balanced Electromagnetic Separation Transducer for Bone Conduction Audiometry and Hearing Rehabilitation

Karl-Johan Fredén Jansson

ISBN 978-91-7597-568-9

This thesis has been prepared using LaTeX.

Doktorsavhandlingar vid Chalmers Tekniska Högskola
Series No 4249.
ISSN 0346-718X

Department of Electrical Engineering
Biomedical Signals and Systems Group
Chalmers University of Technology
SE-412 96 Göteborg, Sweden

tel: +46 31 772 1000
fax: +46 31 772 1783
email: karljohf@chalmers.se

Cover:
A picture of the whiteboard in Karl-Johan's office, filled throughout his time as a PhD student with notes from discussions related to the thesis.

Printed by Chalmers Reproservice
Göteborg, Sweden 2017

Till Sofia ♡

The Balanced Electromagnetic Separation Transducer for Audiometry and Hearing Rehabilitation

Karl-Johan Fredén Jansson
Department of Electrical Engineering
Biomedical Signals and Systems Group
Chalmers University of Technology

Abstract

Hearing via air conduction (AC) and bone conduction (BC) are attributed to be the natural ways of conducting sound to the cochlea. With AC hearing, air pressure variations are transmitted to the cochlea via the ear canal, whereas with BC hearing, sound vibrations are transmitted through the skull bone to the cochlea. Patients with a hearing loss in the cochlea or auditory nerve are commonly rehabilitated with conventional AC hearing aids in the ear canal, but also using cochlear implants. If the pathway for AC sound to reach the cochlea is obstructed, patients can often benefit from bone conduction devices (BCDs). In order to determine the type and degree of hearing loss, the BC hearing thresholds are measured using a bone conduction vibrator, and then analyzed together with the AC hearing thresholds for the diagnosis and to suggest an appropriate rehabilitation alternative. The motor unit in conventional BCDs and bone vibrators are known to generate high amount of distortion at low frequencies where the Balanced Electromagnetic Separation Transducer (BEST) principle may offer a new era in BC hearing rehabilitation and audiometry.

This thesis combines two BC hearing related topics, where the first topic is an evaluation of a new audiometric bone vibrator, Radioear B81, which is assumed to offer more accurate BC hearing threshold measurements. The second topic is related to a new type of active transcutaneous BCD, called the Bone Conduction Implant (BCI), which leaves the skin intact by using a wireless solution that does not require a permanent skin penetration. Even though the applications are different, both devices use the BEST principle as motor unit in their design.

The audiometric bone vibrator Radioear B81 was found to have an improved performance at low frequencies where it can produce higher output levels with less harmonic distortion than the conventional Radioear B71. In a clinical study of the first six patients, the BCI was found as efficient as already commercially available BCDs, and with the advantage of not needing a skin penetration. In a technical evaluation of the BCI, it was shown to be a mechanically robust design and to tolerate magnetic resonance imaging at 1.5 Tesla.

Keywords: balanced electromagnetic separation transducer, bone conduction, bone vibrator, retention magnet, image artifact, demagnetization, magnetically induced torque, magnetic resonance imaging.

Acknowledgments

I would like to thank my examiner & supervisors, colleagues & co-workers, friends & family & my lovely Sofia.

List of papers

This thesis is based on the following papers.

I Electro-Acoustic Performance of the New Bone Vibrator Radioear B81: A comparison with the conventinal Radioear B71. Fredén Jansson, K-J., Håkansson, B., Johannsen, L. and Tengstrand, T. *International Journal of Audiology*, 2014; 54(5):334-340.

II Vibrotactile Thresholds on the Mastoid and Forehead Position of Deaf Patients Using Radioear B71 and B81. Fredén Jansson, K-J., Håkansson, B., Reinfeldt, S., Fröhlich, L. and Rahne, T. *Ear and Hearing*, Accepted for Publication, April 2017.

III Robustness and Lifetime of Active Transcutaneous Bone Conduction Devices. Fredén Jansson, K-J., Håkansson, B., Reinfeldt, S. and Rigato, C. In Manuscript, 2017.

IV MRI Induced Torque and Demagnetization in Retention Magnets for a Bone Conduction Implant. Fredén Jansson, K-J., Håkansson, B., Reinfeldt, S., Taghavi, H. and Eeg-Olofsson, M. *IEEE Transactions on Biomedical Engineering*, 2014; 61(6):1887-1893.

V Magnetic Resonance Imaging Investigation of the Bone Conduction Implant - a pilot study at 1.5 Tesla. Fredén Jansson, K-J., Rigato, C., Håkansson, B., Reinfeldt, S. and Eeg-Olofsson, M. Medical Devices: Evidence and Research, 2015; 8:413-423.

VI The Bone Conduction Implant - Clinical results of the first six patients. Reinfeldt, S., Håkansson, B., Taghavi, H., Fredén Jansson, K-J. and Eeg-Olofsson, M. *International Journal of Audiology*, 2015 Jun;54(6):408-416.

Other publications by the author, not included in the thesis:

- The Bone Conduction Implant - First Implantation, Surgical and Audiologic Aspects. Eeg-Olofsson, M., Håkansson, B., Reinfeldt, S., Taghavi, H., Lund, H., Fredén Jansson, K-J., Håkansson, E. and Stalfors, J. *Otology & Neurotology*, 2014; 35(4):679-685.

- Evaluation of Bone Tissue Formation in a Flat Surface Attachment of a Bone Conduction Implant - A pilot study in a sheep model. Eeg-Olofsson M., Johansson C.B., Lith A., Håkansson B., Reinfeldt S., Taghavi H., and Fredén-Jansson, K.J. *Audiology & Neurotology Extra*, 2014; 4(3):62-76.

- Audiometric Comparison Between the First Patients with the Transcutaneous Bone Conduction Implant and Matched Percutaneous Bone Anchored Hearing Device Users. Rigato, C., Reinfeldt, S., Håkansson B., Fredén-Jansson, K.J., Hol, M., and Eeg-Olofsson, M. *Audiology & Neurotology*, 2016;37(9):1381-1387.

- Touch and Hearing Mediate Osseoperception. Clemente, F., Håkansson, B., Cipriani, C., Wessberg, J., Kulbacka-Ortiz, K., Brånemark, R., Fredén Jansson, K-J. and Ortiz-Catalan, M. *Scientific Reports*, Accepted for publication, 2017.

Please note
Parts of Paper I to VI have been presented in conferences as follows:

- Fredén Jansson, K-J., Håkansson, B., Johannsen, L. and Tengstrand, T. (2013). "A New Audiometric Bone Conductor - B81 for more accurate hearing results," S2 Workshop, Chalmers University of Technology, Department of Signals and Systems, Göteborg, Sweden.

- Fredén Jansson, K-J., Håkansson, B., Reinfeldt, S., Taghavi, H. and Eeg-Olofsson, M. (2013). "MRI induced torque and demagnetization in retention magnets for Bone Conduction Implants," Osseo 2013 4^{th} International Symposium on Bone Conduction Hearing - Craniofacial Osseo-integration, Newcastle, UK.

- Fredén Jansson, K-J. (2014). "The Electro-Acoustic Performance of the New Bone Vibrator Radioear B81 - a comparison with the conventional Radioear B71", AudiologyNOW! 2014 Experience the Magic - AAA, Florida, Orlando, USA.

- Fredén Jansson, K-J., Håkansson, B. and Reinfeldt, S. (2014). "Electro-Acoustic Performance of the New Bone Vibrator Radioear B81 - a comparison with the conventional Radioear B71," Medicinteknikdagarna, Göteborg, Sweden.

- Fredén Jansson, K-J., Håkansson, B. Reinfeldt, S. and Rigato, C. (2014). "MRI Induced Torque and Demagnetization in Retention Magnets for a Bone Conduction Implant," Medicinteknikdagarna, Göteborg, Sweden.

- Fredén Jansson, K-J., and Taghavi, H. (2014). "MRI Induced Torque and Demagnetization in Retention Magnets for Bone Conduction Implants," Svensk Teknisk Audiologisk Förening (STAF), Halmstad, Sweden.

- Fredén Jansson, K-J., and Taghavi, H. (2014). "Nya Audiometriska Benledaren Radioear B81 - en elektroakustiskt jämförelse med Radioear B71," Svensk Teknisk Audiologisk Förening (STAF), Halmstad, Sweden.

- Fredén Jansson, K-J. (2014). "MRI Induced Torque and Demagnetization in Retention Magnets for a Bone Conduction Implant," ISMRM/SMRT Workshop on Safety in MRI: Guidelines, Rationale & Challenges, Washington, D.C., USA.

- Fredén Jansson, K-J. (2015). "Electro-Acoustic Performance of the New Bone Vibrator Radioear B81 - a comparison with the conventional Radioear B71," TeMA Hörsel 2015, Malmö, Sweden.

- Fredén Jansson, K-J., Reinfeldt, S. and Rigato, C. (2015). "MRI Investigation of the Bone Conduction Implant - a pilot study at 1.5 Tesla ," TeMA Hörsel 2015, Malmö, Sweden.

- Fredén Jansson, K-J. and Håkansson, B. (2015). "Electro-Acoustic Performance of the New Bone Vibrator Radioear B81 - a comparison with the conventional Radioear B71," Osseo 2015 5^{th} International Congress on Bone Conduction Hearing and Related Technologies, Lake Louise, Alberta, Canada.

- Fredén Jansson, K-J., Håkansson, B. Reinfeldt, S., Rigato, C. and Eeg-Olofsson, M. (2015). "MRI Investigation of the Bone Conduction Implant - a pilot study at 1.5 Tesla ," Osseo 2015 5^{th} International Congress on Bone Conduction Hearing and Related Technologies, Lake Louise, Alberta, Canada.

- Fredén Jansson, K-J. (2016). "Den audiometriska benledaren Radioear B81 och taktila tröskelmätningar på totalt bilateralt döva," Svensk Teknisk Audiologisk Förening (STAF), Sundsvall, Sweden.

- Fredén Jansson, K-J., Håkansson, B. and Reinfeldt, S. (2017). "Mekaniska tester av och livstidsuppskattning av BCI," Svensk Teknisk Audiologisk Förening (STAF), Göteborg, Sweden.

- Fredén Jansson, K-J., Håkansson, B. and Reinfeldt, S. , Fröhlich, L. and Rahne, T. (2017). "Vibrotactile Thresholds on the Mastoid and Forehead Position of Deaf Patients Using Radioear B71 and B81," Osseo 2017 6^{th} International Congress on Bone Conduction Hearing and Related Technologies, Nijmegen, The Netherlands.

- Fredén Jansson, K-J., Håkansson, B. and Reinfeldt, S. (2017). "Robustness and Lifetime of Active Transcutaneous Bone Conduction Implants," Osseo 2017 6^{th} International Congress on Bone Conduction Hearing and Related Technologies, Nijmegen, The Netherlands.

Contents

Abbreviations and Acronyms

AC	Air Conduction
AM	Amplitude Modulation
ABR	Auditory Brainstem Response
AP	Audio Processor
APHAB	Abbreviated Profile of Hearing Aid Benefit
ASTM	American Society for Testing Materials
BAHA	Bone Anchored Hearing Aid
BEST	Balanced Electromagnetic Separation Transducer
BC	Bone Conduction
BCD	Bone Conduction Device
BCI	Bone Conduction Implant
dB	Decibel
dB HL	Decibel Hearing Level
GBI	Glasgow Benefit Inventory
GE	Gradient-Echo
MR	Magnetic Resonance
MRI	Magnetic Resonance Imaging
PA	Power Amplifier
RF	Radio Frequency
SE	Spin-Echo
SNHL	Sensorineural Hearing Loss
SPL	Sound Pressure Level
SSD	Single Sided Deafness
THD	Total Harmonic Distortion
VSB	Vibrant Soundbridge
VEMP	Vestibular Evoked Myogenic Potential

Part I

Introductory chapters

Chapter 1

Introduction

The natural ways through which the cochlea is stimulated by sound are via air conduction (AC) and bone conduction (BC) hearing. In BC hearing, the cochlea is stimulated from vibrations in the skull bone, whereas in AC hearing, from air pressure variations entering the outer ear. Diagnostic hearing investigations of patients with suspected hearing loss normally comprise both AC and BC hearing threshold testing. In BC threshold testing, sound vibrations are induced in the skull bone by a BC vibrator placed on the mastoid process part of the temporal bone behind the ear, and sometimes on the forehead, to assess the degree of sensorineural hearing loss. When AC hearing is tested, the sound is typically applied by headphones incorporating two small speakers, one for each ear. The difference between the AC and BC thresholds determines the so called air-bone gap, which is commonly interpreted as the degree of conduction hearing loss. If a patient has both a conductive and sensorineural hearing loss, the patient is said to suffer from a mixed hearing loss. Patients with conductive or mixed hearing loss are more likely to benefit from rehabilitation using a bone conduction device (BCD), which stimulates the cochlea by converting AC sound into mechanical vibrations in the skull bone. Rehabilitation of pure sensorineural hearing loss is commonly done by using conventional AC hearing aids with a speaker worn in the entrance of the ear canal. Patients who do not benefit from neither AC nor BC devices due to a profound sensorineural hearing loss can often be rehabilitated using cochlear implants (CIs).

For BC audiometry, the most frequently used BC vibrator has for a long time been the Radioear B71 (Radioear Corporation, Pennsylvania, USA), which was introduced in 1973 (Radioear, 2015c). Even though the B71 has been updated with minor changes over the years, it has always used the conventional variable reluctance type transducer principle, which has well-known limitations at low frequencies where it generates high harmonic distortion at high hearing levels (Håkansson, 2003). The latest version was released under the trade name B71W and is a modified version of B71 to comply with the RoHS directive 2011/65/EU (Radioear,

2015a). To overcome some of these drawbacks, the development of a new BC vibrator resulted in a new transducer principle that generates less harmonic distortion (Håkansson, 2003), sold under the trade name Radioear B81 by Interacoustics A/S (Middelfart, Denmark). The Radioear B81 is based on the Balanced Electromagnetic Separation Transducer (BEST) principle, originally developed at Chalmers University of Technology (Göteborg, Sweden) and further developed and optimized for efficient serial production in collaboration with Ortofon A/S (Nakskov, Denmark). Furthermore, the B81 is designed to replicate the frequency response shape and electrical characteristics of the B71 in order to be compatible with the same type of audiometers.

For rehabilitation using BCDs, the trend in recent years has been towards the development of implantable devices that offer new benefits for the patients. However, these devices have also introduced some new challenges. One challenge is to make the implants relatively small, but still sufficiently powerful. Another challenge is to safely perform magnetic resonance imaging (MRI) in patients with implantable BCDs. One example of such a new implantable BCD is the Bone Conduction Implant (BCI), developed at Chalmers University of Technology and Sahlgrenska University Hospital, both located in Göteborg, Sweden. For the BCI, there is a great interest to investigate how its magnetic and electric conductive materials interact with the MRI scanner, both from a diagnostic and patient safety perspective.

This thesis combines studies on the B81 and the BCI, which both use the BEST principle as motor unit to create vibrations in the skull bone, and the design is comprehensively described in Chapter 3.1.4. The BEST principle improves the poor low frequency performance of conventional transducers and at the same time offers a more efficient, lighter and smaller design that is suitable for implantation. Generally speaking, the BEST principle is a balancing technique that improves linearity so that harmonic distortion is reduced.

The BEST transducer in the BCI is much smaller than in the B81, has other frequency characteristics and is hermetically encapsulated in order to be suitable for permanent implantation. It is implanted in a 3-5 mm deep recess drilled in the mastoid part of the temporal bone to give a direct bone drive with no soft tissues in-between. In comparison with a BC vibrator attached over the skin with a static pressure, the resonance peaks in the frequency response of the BCI transducer need to be damped when the transducer is driven directly on a bone surface to avoid problems with feedback stability. A wireless link supplies the transducer with a sound signal from an audio processor that is magnetically attached over the skin to the patient′s head. By leaving the skin intact, the risks for skin complications, such as those from skin penetrating implants, are reduced. In an ongoing clinical study, approved by the Swedish Medical Agency and the regional Ethical Review Board, it can be seen that the BCI offers a significant hearing rehabilitation for patients with conductive or mild-to-moderate mixed hearing loss. Furthermore, studies of the MRI safety of the BCI have been conducted and the results show

that the present design is likely to pass a conditional approval to be worn in a 1.5 Tesla MRI scanner. Also, mechanical tests have verified the implant to be robust, and in a long-term age acceleration test, its lifetime was estimated to be at least 10 years without any noticeable effects on its electro-acoustic performance.

1.1 Aim of thesis

The overall aim of this thesis is to evaluate two new devices used in the field of bone conduction audiometry and hearing rehabilitation: the BC vibrator Radioear B81 and the BCI system.

In Papers I and II, the aim was to evaluate the electro-acoustic performance of the Radioear B81 in comparison with the conventional Radioear B71 and to measure vibrotactile thresholds using both devices. In the papers related to the BCI system (Papers III-VI), the general aim was to verify the mechanical robustness of the implantable unit of the BCI and to investigate its safety and effectiveness as an active transcutaneous BCD for rehabilitation of patients with conductive or mild-to-moderate mixed hearing loss. More detailed, in Paper III, the aims were to develop test methods and criteria for verification of mechanical robustness and lifetime estimation of active transcutaneous BCDs and to apply those to the BCI implant. The aims of Papers IV and V (and partly Paper III) was to investigate the effects and risks related to MRI scanning of patients implanted with a BCI, such as magnetically induced torque, demagnetization, image artifacts, induced sound and its effects on the electro-acoustic performance. Finally, the aim of Paper VI was to present the audiological and patient related outcomes for the first six patients implanted with the BCI by summarizing their audiometric results and measures from two validated questionnaires at the 6-month follow up visit.

1.2 Thesis outline

Followed by the introductory Chapter 1, where the objective and problem descriptions are presented, Chapter 2 describes basic hearing physiology and bone conduction audiometry, as well as gives the principles of MRI. An overview of the devices investigated in this thesis is given in Chapter 3. Appended papers (I-VI) are shortly summarized in Chapter 4 and their most important outcomes are concluded in Chapter 5 together with plans for future studies.

Chapter 2

Basics of audiology and magnetic resonance imaging

2.1 Audiology - a brief overview

The natural function of the peripheral parts of the human ear is to transform airborne sound to nerve signals that are transmitted to higher centres in the brain. This transformation can be explained by dividing the ear into three components: the outer ear, the middle ear and the inner ear. An illustration of the ear anatomy is given in Figure 2.1. The outer ear consists of the pinna and the ear canal, terminated by the tympanic membrane, which serves as an interface between the incoming sound and the middle ear. The middle ear cavity comprises the ossicular chain (malleus, incus and stapes), which transmits the sound induced vibrations of the tympanic membrane further to the oval window, entering into the cochlear fluids of the inner ear. These vibrations are then transformed into a travelling wave in the cochlear fluids causing hair cells on the basilar membrane to generate electrical response signals that are transmitted via the auditory nerve and further to the brain for sound interpretation.

The cochlea can also be stimulated directly from vibrations in the skull bone, for example from a person′s own voice when speaking, or from a transducer that vibrates the bone. Hearing through the ear canal and vibrations in the bone are attributed to air conduction (AC) and bone conduction (BC) hearing, respectively. It was early found by Békésy (1932) that the basilar membrane moves similarly regardless if the sound is conducted via air or bone conduction when he was able to completely cancel the AC sound at the cochlea by applying a BC sound with equal loudness, but opposite phase. In Figure 2.2, the AC and BC pathways are illustrated, both from a vibrating transducer and from a person′s own voice.

People with hearing disorders in the outer, middle or inner ear can suffer from either conductive, sensorineural (SNHL) or mixed hearing loss, depending on where

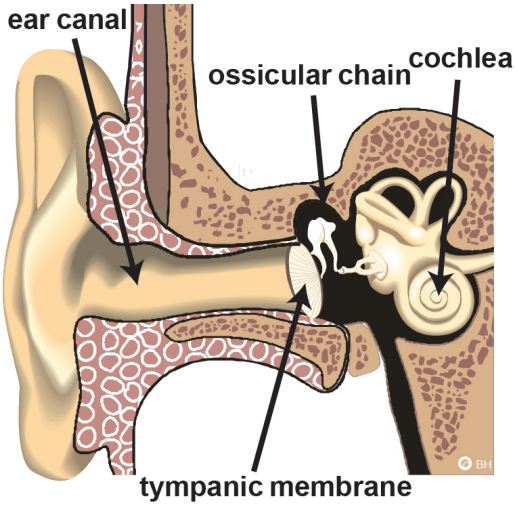

Figure 2.1: The anatomy of the human ear showing the outer ear with the pinnae and the ear canal which is terminated by the tympanic membrane, the ossicular chain constituting the middle ear, and the inner ear with the cochlea.

the disorder is located. Patients who are suffering from conductive hearing loss have a malfunction in the outer and/or the middle ear, while SNHL typically refers to an impairment of the inner ear or the auditory nerve pathway to the brain. A patient who has no sensorineural hearing on either one or both ears is diagnosed as uni- or bilaterally deaf, respectively. Complete deafness on one ear is also commonly referred to as single sided deafness (SSD). From an audiometric point of view, uni- or bilaterally deaf means that patients have unmeasurable hearing thresholds, i.e. the thresholds are unable to reach with a standard audiometer.

2.2 Audiometry and rehabilitation

A patient′s hearing thresholds are documented and illustrated in a so called audiogram, mainly comprising both AC and BC hearing thresholds as well as speech thresholds for left and right ears, and if needed, thresholds may be measured with masking of the contralateral ear. The hearing thresholds are measured using an audiometer that creates sounds at different hearing levels and frequencies for both AC and BC stimulation. When AC hearing is tested, the sound is typically applied by headphones, and when BC hearing is tested, the stimulus is applied with a BC vibrator. The headphones incorporate two small speakers, one for each ear, whereas the BC vibrator is a single unit that is attached (and pressed) towards the skin with a steel spring on the mastoid process part of the temporal bone behind the pinna of the outer ear. The BC vibrator can also be placed on the forehead instead of the mastoid process so that both left and right ear can be stimulated from the same location. After both the AC and BC thresholds have been mea-

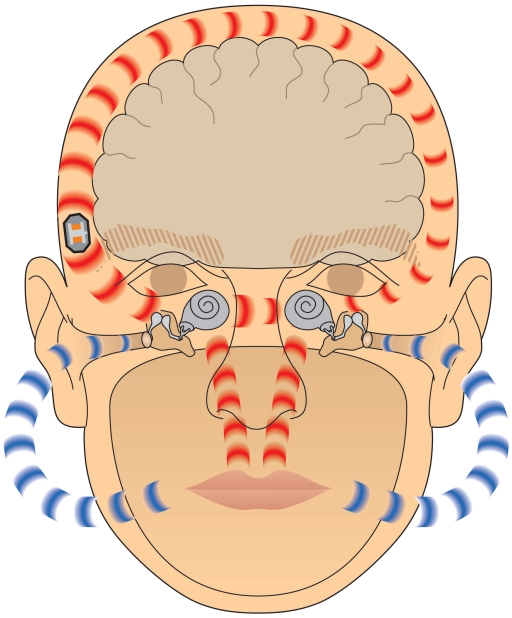

Figure 2.2: An illustration of the air conduction (blue) and bone conduction (red) pathways of the sound from a person′s own voice and an implanted transducer in the temporal bone.

sured, the BC thresholds are compared with normal AC hearing levels to reveal the degree of SNHL, while a conductive hearing loss is found by calculating the air-bone gap, which is the difference between the AC and the BC thresholds.

There are many possible causes of SNHL, but it is most commonly related to aging and noise induced hearing loss i.e. exposure to high sounds that have damaged the hair cells in the inner ear. There are also different classifications of SNHL depending on its severity which varies from slightly (16-25 dB HL) to profound (greater than 90 dB HL). Patients with conductive hearing loss are less frequent than patients with SNHL and have other possible causes, such as chronic ear infections, otosclerosis, and other problems associated with the outer and middle ear (Clark, 1981).

Depending on the severity and type of hearing loss, there are different types of devices for hearing rehabilitation. Hearing loss is commonly rehabilitated with conventional AC hearing aids that amplify the sound directly in the ear canal. However, patients who are unable to use such devices or are suffering from conductive hearing loss are commonly rehabilitated with a bone conduction device (BCD). BCDs are also used to provide rehabilitation for patients with mixed hearing loss or SSD. Patients who does not benefit enough from using neither conventional AC hearing aids nor BCDs, may have damaged sensorineural receptors and does not respond to an increased level of sound. Instead, those patients are typically rehabilitated with cochlear implants (CIs) that, unlike AC hearing aids and BCDs,

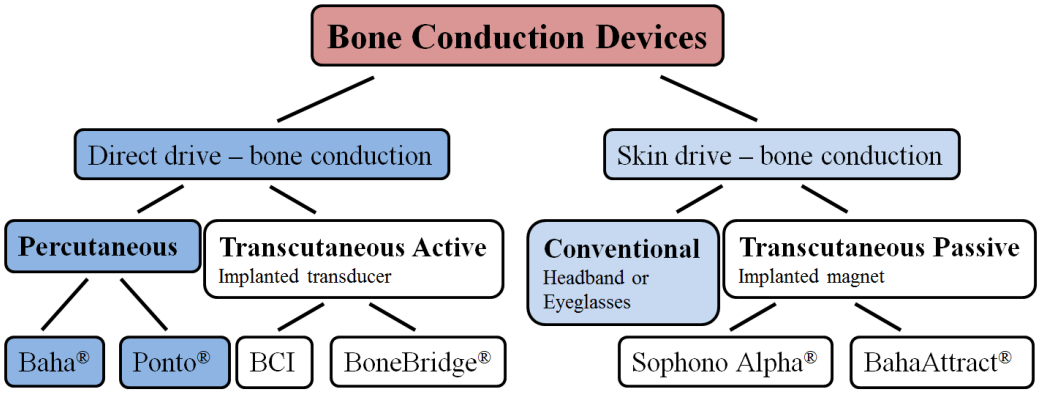

Figure 2.3: Categorization of different bone conduction devices including the BCI and commercial devices available on the market, a modified version of Figure 1 in Reinfeldt et al. (2015a).

use an electrode inserted in the cochlea to provoke nerve signals along the basilar membrane.

However, a if a BCD surgery is needed, it does not involve the same risks as a CI surgery which is more invasive as it requires an electrode to be implanted into the cochlea. When using a BCD, the airborne sound is transformed by an audio processor (AP) to electric signals that drive a vibrating transducer, giving vibrations that are bypassing the outer and middle ear. The categorization of a BCD depends on the position and attachment of the transducer, which is clarified by Figure 2.3 (Reinfeldt et al., 2015a). In conventional BCDs, the transducer is pressed against the skin over the skull bone with a static force. The percutaneous bone anchored hearing aid (BAHA) provides stimulation directly via a skin-penetrating abutment that is anchored to the skull bone by the use of a titanium fixture. Passive and active transcutaneous BCDs use one externally worn AP and an implanted unit under the skin and are thereby skin-intact solutions (Reinfeldt et al., 2015a). Depending on whether the transducer is located in the AP or in the implanted unit, the transcutaneous BCD is said to be either passive or active, respectively. As the trend during recent years has been to develop implantable hearing devices, new materials have been introduced in the body, which raise new questions regarding safety issues. The focus in this thesis is on active transcutaneous BCDs and in particular on the bone conduction implant (BCI) developed in Göteborg, Sweden, with emphasis on aspects concerning magnetic resonance imaging (MRI).

2.3 Safety aspects of magnetic resonance imaging

MRI is used as a diagnostic tool to visualize internal structures and organs of the human body by letting soft tissue and fluids interact with magnetic fields (Bushong, 2003). A patient who is using an implanted medical device should not undergo an MRI examination if it has not been proven to be safe (Shellock, 2012). The reason is that the magnetic fields from the MRI scanner interact with implants containing magnetic or electric conductive materials, which is the case for hearing implants, pacemakers and some prosthetic implants. In order to evaluate the MRI safety of such implants, the magnetic fields of the MRI scanner can be divided into three main magnetic field components: the static field, the radio frequency (RF) field and the gradient field. The associated risks can then be evaluated in more detail by performing separate tests on each field.

Permanent magnets and ferromagnetic materials align with the static field, which induces forces and torques that can cause more or less severe complications, such as implant damage and dislocation, and in the worst case injury to the patient (Teissl et al., 1998). The RF and gradient fields are time-varying fields that can induce electrical currents in electric conductive materials, such as conductive wires, plates and some magnetic materials. Some risks with induced currents are that they can generate heat, damage some electronic components and possibly also cause unwanted stimulation of the implant (Nyenhuis et al., 2005; McComb et al., 2009). The American Standard for Testing Materials (ASTM) has developed guidelines and recommendations on how to evaluate the MRI safety risks regarding implants. After being thoroughly tested, the implant should be labeled either as MR safe, MR unsafe or MR conditional. The latter label is the most commonly used one for implantable BCDs and means that scanning is only allowed under certain conditions (Shellock, 2012).

Today, the only commercially available active transcutaneous BCD is the Bonebridge™ (MED-EL Corp., Innsbruck, Austria), which is approved as MR conditional at 1.5 Tesla. The commercially available passive transcutaneous BCDs are Sophono™ Alpha 2 (Sophono Inc., Denver, USA) which is MR conditional at 1.5 and 3 Tesla, and Baha® Attract (Cochlear BAS, Mölnlycke, Sweden) which is MR conditional at 1.5 Tesla. The Vibrant Soundbridge (VSB) from MED-EL is an active transcutaneous middle ear implant with the transducer attached to the long process of the incus (Jesacher et al., 2010; Beltrame et al., 2009). Compared to BCDs, the transducer in the VSB vibrates the ossicular chain instead of the skull bone and stimulates the cochlea via the oval window. The MRI safety of the VSB has been thoroughly investigated, but only models of its implanted unit released after 2014 has been approved as MR conditional at 1.5 Tesla. (MED-EL, 2014).

2.3.1 The static magnetic field

Soft tissue and fluids inside the human body consist of hydrogen atoms, which have gyromagnetic properties. The purpose of the static field is to magnetize the human body in one direction by aligning hydrogen protons in a gyroscopic rhythm with precision, referred to as equilibrium. This will make the aligned protons to rotate with a deflection angle around the equilibrium direction in a gyroscopic motion. The amount of aligned magnetization M and the frequency of rotation will depend on the magnetic flux density B_0 of the static magnetic field of the MRI scanner, which is given in the unit Tesla. The rotation frequency is commonly referred to as the Larmor frequency f_L and is calculated as

$$f_L = \frac{\gamma}{2\pi} B_0, \tag{2.1}$$

where $\gamma/2\pi$ is the gyromagnetic constant, which is 42.6 MHz/Tesla for hydrogen (Bushong, 2003). This means that f_L is approximately 64 and 128 MHz for 1.5 and 3 Tesla MRI scanners, respectively. According to Boltzmann′s distribution (Haacke et al., 1999), the stronger the static magnetic field is, the stronger will the magnetization signal for a proton density ρ be at temperature T according to

$$M = \frac{\rho \gamma^2 h^2}{16\pi^2 k_b T} B_0. \tag{2.2}$$

A stronger signal is an advantage in terms of resolution, acquisition time and signal to noise ratio. However, a higher B_0 requires that the RF coils can work at higher frequencies, and most importantly, the magnetically induced torque Γ on implants that contain magnetic materials will increase. The magnetic torque can be approximated as

$$\Gamma = m B_0 sin\theta, \tag{2.3}$$

where θ is the angle between the direction of the static magnetic field of the MRI scanner and the magnetic moment m of the implant (Coey, 2010; Todt et al., 2011).

2.3.2 The radio frequency field

Once the body is magnetized in the direction of the static magnetic field, a RF field is applied to manipulate the magnetization. The RF field is a sequence of RF pulses with energy at the Larmor frequency to excite the gyroscopic motion of the magnetization. This will cause the deflection angle to increase and the magnetization to deviate from equilibrium, and the time it takes for it to fall back again is measured. The time it takes for the magnetization to fall back to equilibrium is called the relaxation time and varies for different types of tissues with different hydrogen densities. Different types of pulse sequence are used for scanning with specific pulse combinations in time, direction and, together with gradient

fields, at specific locations. The RF field is applied and measured simultaneously using different coil types, specially designed for scanning of the whole body, knee or head (Bushong, 2003).

2.3.3 The gradient field

The gradient field is used to excite the magnetization at different locations in the body by creating a gradient in the static magnetic field. This makes the Larmor frequency specific at different locations over the body. By switching the gradient for different locations, response signals can be distinguished from different locations in the body and collected as data for image reconstruction. The switched gradient fields should not be confused with the spatial gradient field, which is static and caused by the uniform field inside the bore as it decays around the scanner (Shellock et al., 2011).

2.4 Mechanical safety aspects

The mechanical robustness and lifetime of the implanted unit of a transcutaneous BCD relates to the safety of the device since an explantation of a damaged or broken device requires surgery, which is a risk in itself. It is therefore not only important to ensure that the device can withstand MRI, but also that it can withstand the mechanical stress that it possibly will be exposed to during daily life activities. Furthermore, it is important to know that the device will continue to function as intended for a long period of time in order to avoid the need for re-implantation. Different types of BCDs may be more or less robust depending on their categorization and how exposed they are to external impacts. In percutaneous devices, the implant is fully exposed as it sticks out of the skin, while transcutaneous devices, both active and passive, are protected by the skin over the implant. The main difference between passive and active devices is that the transducer in an active device is implanted, while in a passive device it is worn externally. Therefore, there are higher demands on the robustness of the transducer design of the active devices than of the passive. Replacement of a broken transducer that is externally worn can easily be done by changing the AP, which is a safe procedure as it does not involve any surgery.

The association for the advancement of medical instrumentation (AAMI) have developed tests for evaluating the mechanical robustness of CIs. The ones out of those tests, also relevant to use when evaluating the mechanical robustness of active transcutaneous BCDs are comprehensively described in Paper III and summarized below:

- **Mechanical shock test:** A half-sine mechanical pulse with a duration of 1 ms and a peak of 500 g is applied in five orthogonal directions (excluding the feedthrough side) to the implant by attaching it to a device holder being

dropped in a pendulum motion onto a wall. This test applies shocks that the implant may be exposed to throughout the patients' lifetime as well as when being handled prior to or during surgery.

- **Random vibration test:** A band limited white noise with a power spectral density of 0.7 $(\mathrm{m}/s^2)^2/\mathrm{Hz}$ from 5 to 500 Hz is applied in three orthogonal planes for 30 minutes in each plane by using a mini-shaker. This test applies vibrations to the implant that it may be exposed to throughout the patients' lifetime as well as when being handled prior to or during surgery.

- **Drop test:** The implant is dropped twice in three perpendicular directions at a hight of 1 meter onto a 50 $\pm$ 5 mm thick hardwood surface having a density greater than 600 $\mathrm{kg/m^3}$, lying flat on a concrete or a similar rigid surface. This test may not be as relevant for an implanted transducer as for an externally worn device, because if an implant is by accident dropped on the floor, it is no longer sterilized and should not be implanted. If the implant is dropped during transportation after production, it is commonly packed in a box and surrounded by some material that will protect it from excessive mechanical exposure.

- **Pendulum test:** As an alternative to the drop test, a pendulum arm can be used to strike the implant in a controlled direction and with an exact force for different floor materials. To mimic an accidental drop onto a sterilized surgery table made of metal, the pendulum rod with a stiff metal surface may be dropped from a height of maximum 50 cm to strike the implant. Five orthogonal sides (not the feedthrough side) are tested. By controlling the direction and force using a pendulum arm, effects from rebouncing, air-resistance and random striking side are neglected in this test.

- **Mechanical impact test:** The side of the implant facing out from the skull bone when implanted in patients is exposed to an impact of 2.5 Joule, established by dropping a spherical metal weight with a mass of 1.622 kg from a height of 15.7 kg. During the test, the implant rests on a firm and solid surface, similar to how it is implanted in a patient and a 3 mm silicon sheet covers the test side to represent the skin. This test is relevant for evaluating the effects from external impacts during more extreme situations, such as hits to the head over implant from accidents or sport activities.

- **Age-acceleration test:** At the same ambient conditions as for an implanted device, the complete device is exposed to higher sounds and for a longer period of time than during normal operation in order to accelerate the ageing effect and estimate the expected lifetime of the device. In comparison with the random vibration test where the vibrations are externally applied, the age-acceleration test also evaluates the robustness towards the transducer's selfinduced vibrations in one plane.

To evaluate the effects on the implant from each test, the electro-acoustic performance should be measured before and after each test and relevant criteria for maximum acceptable changes from nominal response should be set for each device.

Chapter 3

Devices

3.1 Bone conduction vibrators

Diagnostic hearing investigations of patients with suspected hearing loss comprise both air- (AC) and bone conduction (BC) hearing threshold testing. A BC vibrator is a device that applies the sound when BC hearing thresholds are measured. The vibrator is attached to the skin over the mastoid process part of the temporal bone or on the forehead, using a steel spring, and it is driven by a calibrated audiometer to generate hearing levels at different frequencies.

3.1.1 Radioear B71

The B71 from Radioear (Radioear Corporation, Pennsylvania, USA) has been the most widely used BC vibrator since the 1970′s (Gallichan et al., 1998) and is shown in Figure 3.1. Recently, Radioear released the B71W, which has practically identical performance as the B71, but does not contain any lead in order to comply with the RoHS directive 2001/65/EU (Radioear, 2015a). Examples of other BC vibrators developed over the years are, from Radioear, the B70 and the B72, and from Grahnert Präcitronic GmbH (Dresden, Germany), the KH70. The Radioear devices are characterized by their three distinct but damped resonance peaks, while the KH70 only has one low frequency peak, but a flat and smooth frequency response at higher frequencies (Richards and Frank, 1982). Furthermore, the KH70 has the advantage that it radiates less airborne sound, but is large and heavy, which makes it hard to attach behind the ear without touching the pinna (Håkansson, 2003; Stenfelt and Goode, 2005).

Even though the B71 is the standard BC vibrator, it has some well-known limitations in its performance at low frequencies where it generates a large amount of non-linear distortion at higher hearing levels. Over the years, this has led to the fact that BC hearing thresholds are rarely tested below 500 Hz using the B71

Figure 3.1: External view of the Radioear B71.

because of the inherent second order harmonic distortion of variable reluctance type transducers. A comprehensive description of the variable reluctance type transducer is given in Håkansson (2003) and is summarized in section 3.1.2.

3.1.2 The variable reluctance type transducer

The variable reluctance type transducer in the Radioear B71 is electromechanically transmitting vibrations to its housing when it is driven by a time-varying current, *i(t)*. This current flows through a pair of twin coils that are winded around two yoke arms to create a time-varying flux, $\Phi_{\sim}$, in thin air-gaps, see Figure 3.2.

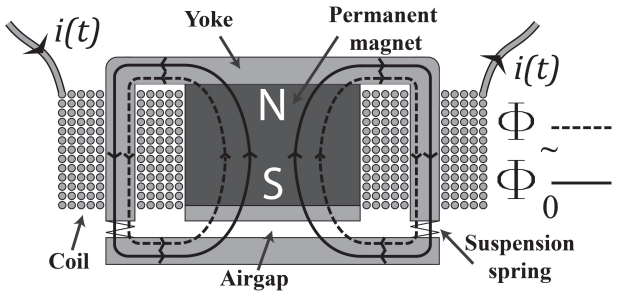

Figure 3.2: Cross-sectional view of the variable reluctance transducer in the B71 bone conduction vibrator.

A permanent magnet with a static magnetic flux, Φ_0, is positioned between the twin coils to achieve a static force in the thin air-gaps that is maintained using a counteracting suspension spring. When $\Phi_{\sim}$ varies, the air-gap will change its width accordingly to $\Phi_{\sim}$ and the total vibrating force, F_{tot}, of the transducer will be proportional to the total magnetic flux in the air-gap squared so that

$$F_{tot} \propto (\Phi_0 + \Phi_{\sim})^2 = \Phi_0^2 + 2\Phi_0\Phi_{\sim} + \Phi_{\sim}^2. \tag{3.1}$$

From equation 3.1 it can be seen that F_{tot} is nonlinearly depending on $\Phi_{\sim}$. For small values of $\Phi_{\sim}$ (i.e. $\Phi_{\sim} << \Phi_0$), where the nonlinear effect is negligible and

$2\Phi_0\Phi_\sim$ is much greater than $\Phi_\sim^2$. For higher values of $\Phi_\sim$, harmonic distortion will be noticeable, especially at low frequencies, which causes an accuracy problem in BC audiometry. In order to minimize this nonlinear effect, a permanent magnet with a high static magnetic flux Φ_0 is needed that also will give a static force in the air-gap. This will require a stiffer suspension spring to maintain the air-gap, but a stiffer spring will also move the vibrator resonance peak to a higher frequency according to equation 3.2. Unfortunately, a relatively low resonance frequency is required in BC audiometry and can only be regained by increasing the counteracting mass, m, making the BC vibrator heavier. One such example is the Radioear B72, which is a modified version of B71 that has been designed with a higher mass and larger casing to increase the output at low frequencies (Radioear, 2015b). The vibrator resonance frequency, f_r, can be approximated to a function of the mass m and the spring stiffness k as

$$f_r \approx \frac{1}{2\pi}\sqrt{\frac{k}{m}}. \tag{3.2}$$

3.1.3 Radioear B81

To overcome the issues with distortion at low frequencies, a new type of BC vibrator has been developed at Chalmers University of Technology (Göteborg, Sweden) in collaboration with Ortofon A/S (Nakskov, Denmark), and is now sold under the trade name Radioear B81 by Interacoustics A/S (Middelfart, Denmark), see Figure 3.3. Its motor unit is based on the balanced electromagnetic separation transducer (BEST) principle, which was first invented by Håkansson (2003) in an attempt to improve the performance of conventional transducers and to make them smaller and more suitable to be used in hearing implants. The BEST principle was also found beneficial for BC audiometry as it was discovered to have an improved performance at low frequencies, where improvements are called for. A comprehensive description of the BEST principle is given in Håkansson (2003) and is summarized in section 3.1.4.

Figure 3.3: External view of the Radioear B81.

3.1.4 The balanced electromagnetic separation transducer

The balanced electromagnetic separation transducer (BEST) principle is also a variable reluctance type transducer, but it uses four permanent magnets positioned in a way that the static as well as the non-linear harmonic forces are opposed and cancelled. This is achieved by a balance between two inner and two outer air-gaps. In each air-gap, a permanent magnet contributes with a static flux, Φ_0, and in the inner air-gaps, an additional time-varying flux, $\Phi_\sim$, is induced as a current flows through a coil winded around a bobbin core. The inner air-gaps are one upper and one lower, where Φ_0 are opposed in direction by the permanent magnets mounted with opposed magnetization direction, but $\Phi_\sim$ flows in a closed loop through each air-gap, creating the dynamic force. An illustration of the magnetic circuit of the BEST principle is shown in Figure 3.4, where A and D are the outer air-gaps while B and C are the inner air-gaps.

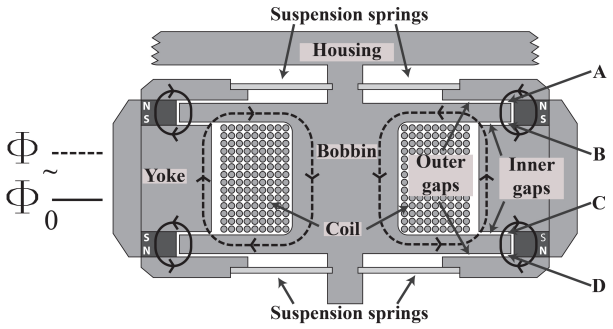

Figure 3.4: Cross-sectional view of the BEST design showing its permanent magnets and air gaps.

The time-varying and static flux pathways are outlined by dashed and solid lines, respectively, and it can be seen that half of the time-varying flux flows through each side. As the force in each air-gap is proportional to the total flux in the air-gap squared, the total flux to force relation of the transducer can be found by calculating the force proportionality in each air-gap and adding them together. Moreover, the forces in air-gap A and D are

$$F_A = -F_D \propto \Phi_0^2, \tag{3.3}$$

and in air-gap B

$$F_B \propto (\Phi_0 - \frac{\Phi_\sim}{2})^2, \tag{3.4}$$

and in air-gap C

$$F_C \propto -(\Phi_0 + \frac{\Phi_\sim}{2})^2. \tag{3.5}$$

Using the symmetry for both sides, the total vibrating force of the transducer can be found by multiplying the force on one side by a factor of 2 as follows

$$F_{tot} = 2(F_A + F_B + F_C + F_D). \tag{3.6}$$

Finally, by inserting equations 3.3 to 3.5 in equation 3.6, the total vibrating force is proportional to

$$F_{tot} \propto 2(\Phi_0^2 + (\Phi_0 - \frac{\Phi_\sim}{2})^2 - (\Phi_0 + \frac{\Phi_\sim}{2})^2 - \Phi_0^2) = 4\Phi_0\Phi_\sim. \tag{3.7}$$

It is obvious from equation 3.7 that the flux to force relation is linear as both the static term Φ_0^2 and the second order distortion term $\Phi_\sim^2$ have been cancelled. To clarify, this explains why the total harmonic distortion is much lower for the B81 in comparison with the conventional B71.

3.2 Bone conduction devices

The various types of bone conduction devices (BCDs) summarized in Figure 2.3 are explained in more detail in this section.

3.2.1 Conventional devices

The only BCD type that does not require any surgery is the conventional BCD. In such systems, a transducer is pressed against the skin in order to vibrate the skull bone. A static force, typically higher than 2 Newtons, is required for efficient transmission of sound and is accomplished either using a steel spring or a soft head band, see Figure 3.5. This is the same principle that is used by audiometric BC vibrators except that the transducers in BCDs are driven by a battery operated audio processor (AP) instead of a power line operated audiometer. Unfortunately, it is very annoying to have a constant force of 2 Newtons or more during a longer period of time if the device is worn on a daily basis. Another challenge is to handle feedback issues at high gain settings, which in the worst case require the microphones to be positioned on the contralateral ear or in a body worn pocket. Furthermore, the skin attenuates the higher end of speech frequencies, which limits the rehabilitation in patients with mixed hearing loss when higher gain is needed (Håkansson et al., 1984).

3.2.2 The bone anchored hearing aid

In the late 1970′s, the percutaneous bone anchored hearing aid (BAHA) was developed to overcome some of the issues with skin driven conventional BCDs. Its transducer and microphones are housed in the same unit and attached to a skin-penetrating abutment that is anchored in the skull bone using a titanium fixture,

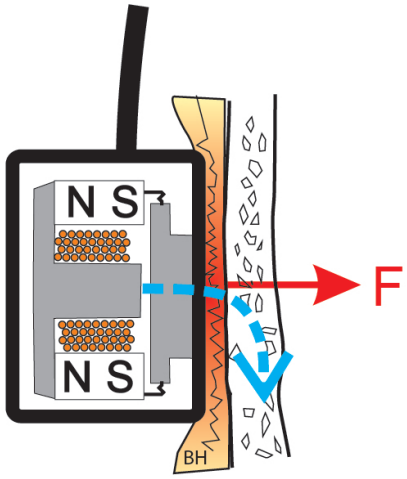

Figure 3.5: An illustration of the conventional bone conduction device that induces vibrations to the skull bone by a transducer that is pressed against the skin with a static force F using a steel spring (Håkansson, 2011).

see Figure 3.6 (Håkansson et al., 1985; Lidén et al., 1990; Tjellström et al., 2001). Similar to dental implants, the titanium fixture is drilled into the bone to achieve an osseointegrated attachment. The surgery is quick and safe and has been improved over the years by introducing new techniques to reduce skin complications (de Wolf et al., 2008; Hultcrantz and Lanis, 2014). In comparison with conventional BCDs, the BAHA offers a direct drive to the bone and thereby a more efficient transmission of high frequency sounds (Håkansson et al., 1984). As the high frequency performance is improved, both patients with conductive and mild-to-moderate mixed hearing loss can benefit from this device. However, some skin complications can arise around the skin-penetrating abutment and this area requires daily care (Snik et al., 2005; Dun et al., 2012; Kiringoda and Lustig, 2013). Also, the challenge with feedback remains (Taghavi et al., 2012), even though it is not as critical as for conventional BCDs.

3.2.3 Transcutaneous devices

Even though, conventional and percutaneous BCDs are still widely used, the trend towards transcutaneous (intact skin) solutions that reduce skin-related complications has increased. Both passive and active solutions are commercially available on the market. The passive solutions are very similar to conventional BCDs, with the vibrations transmitted through the skin, but where the static retention force is established using permanent magnets instead of a steel spring or headband, see Figure 3.7. Even though the skin is intact, the high frequency damping of the skin remains, feedback control is still a challenge and a relatively high retention force is required for efficient sound transmission. This may compress the skin and soft

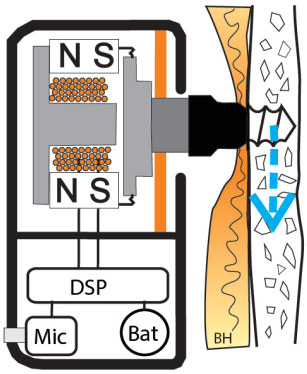

Figure 3.6: The percutaneous bone anchored hearing aid. It uses a battery driven transducer and audio processor unit coupled to a skin penetrating abutment screw that is fixed in the skull bone to achieve an osseointegrated and direct bone drive. A microphone picks up the sound and a digital sound processor adjusts the input and drives the transducer (Håkansson, 2011).

tissue to the extent that there is a risk for skin complications caused by limited nutrition supply to soft tissue in that region.

In active transcutaneous BCDs, the transducer casing is directly attached to the bone, achieving a direct bone drive as in the BAHA, but the skin is kept intact. Instead, the sound is wirelessly transmitted as an amplitude modulated electromagnetic carrier signal from a transmitter coil in the AP to a receiver coil in the implanted unit. The current in the receiver coil will then be demodulated back to the original signal, which will directly drive the implanted transducer. To optimize the signal transmission of the link, the two coils are separately tuned and the retention force is accomplished by using one permanent magnet in the center of each coil. The retention force is here significantly less than in conventional and passive transcutaneous BCDs (typically less than 1 Newton) as the external unit is of relatively light weight and since there is no need to promote vibration transmission through the skin. Also, the microphones in active transcutaneous BCDs are well separated from the transducer and with skin in-between, which makes these BCDs less prone to feedback.

3.2.4 The bone conduction implant

The bone conduction implant (BCI) is an active transcutaneous BCD developed in Göteborg, Sweden, by research groups at Chalmers University of Technology and Sahlgrenska University Hospital (Håkansson et al., 2010; Eeg-Olofsson et al., 2014; Reinfeldt et al., 2015b; Taghavi et al., 2015). It is currently under evaluation and verification in an ongoing clinical study approved by the Swedish Medical Agency and the Regional Ethical Review Board. The papers included in this thesis indicate that the BCI is safe for the patients and that it provides a viable rehabilitation

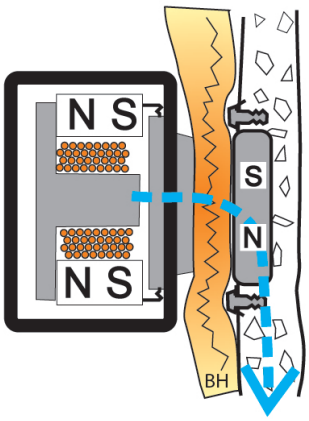

Figure 3.7: The principle design of a passive transcutaneous bone conduction device, where the vibrations are transmitted to the bone via the skin as similar to the conventional BCD except that it uses implanted magnets for retention instead of a steel spring or soft headband (Håkansson, 2011).

alternative for patients who are suffering from conductive or mild-to-moderate mixed hearing loss, and that it possibly tolerates magnetic resonance imaging at 1.5 Tesla.

The vital components of the BCI implant (transducer, electronics, and retention magnet) are sealed in a hermetic titanium casing and the whole implant is sealed by an implant-grade silicon, except the medial facing titanium surface in contact with the skull bone for osseointegration. In Figure 3.8a, the principal design of the BCI system is shown and in Figure 3.8b the external view of the AP and the implanted unit are shown. By the use of a wireless induction link, a current is induced in the receiver coil to drive the transducer. The transducer is based on the BEST principle and is attached inside the titanium casing in a way that a high resonance frequency is created. The transducer casing is mounted in a 3-5 mm deep drilled recess of the mastoid process part of the temporal bone in order to establish a flat surface attachment to the bone. Currently, the transducer casing is fixed by a titanium wire, but also other methods might be used, such as a titanium bar or sutures.

The AP comprises two microphones, a digital signal processor, amplitude modulation electronics, a retention magnet and a transmitter coil (Taghavi et al., 2015). Incoming sound to the microphones are transformed to an electrical signal, processed by digital filters and compressors, and then amplitude modulated to finally be transmitted via a carrier wave through the induction link to the implant. After the amplitude modulated signal has been received by the receiver coil, it is first demodulated from the carrier wave back to the original sound signal and then fed directly to the transducer.

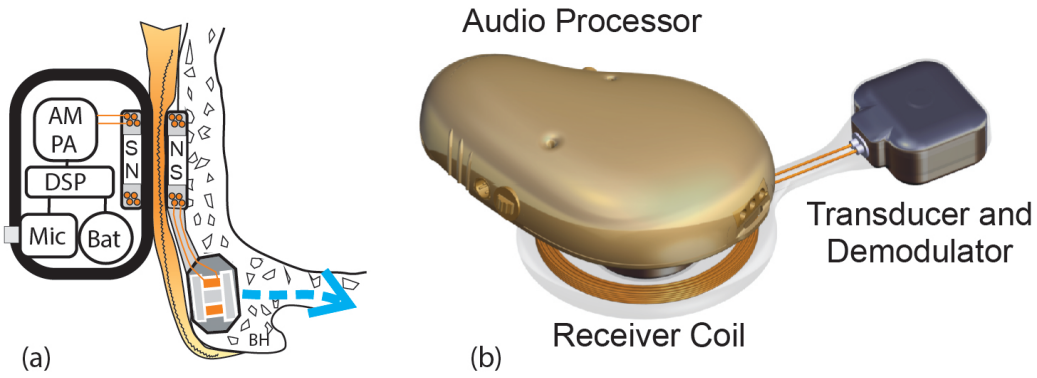

Figure 3.8: a) An illustration of the principal design and the components of the BCI system showing the audio processor with microphone, digital sound processor, power amplifier, amplitude modulation circuits, induction link and transducer (Håkansson, 2011). b) The external view of the BCI system being used in the ongoing clinical study (Reinfeldt et al., 2015b).

Chapter 4

Summary of papers

4.1 Electro-acoustic performance of the new bone vibrator Radioear B81: A comparison with the conventional Radioear B71 (Paper I)

The objective of the study presented in Paper I was to evaluate the electro-acoustic performance of the B81 in comparison with the B71. Frequency response, total harmonic distortion (THD), maximum output and electrical impedance were measured for six devices of each bone conduction (BC) vibrator type on an artificial mastoid Brüel & Kjær 4930, where the BC vibrators were attached with a static force of 5.4 N according to ISO 389-3 (1994). However, the B71 is known to produce high distortion at low frequencies due to its conventional design with unbalanced air gaps. In an attempt to improve the low frequency performance, the balanced electromagnetic separation transducer (BEST) principle was suggested to be used as the motor unit in audiometric BC vibrators by Håkansson (2003). The BEST principle comprises two opposed, but statically balanced, air gaps so that non-linear distortion is reduced and higher output levels can be achieved. In a collaboration between Ortofon A/S (Nakskov, Denmark) and Chalmers University of Technology (Göteborg, Sweden), the BEST design has been further optimized. Essentially, it is adapted for serial production as it serves as the motor unit of the new bone vibrator Radioear B81.

For compatibility with the same type of audiometers, the frequency response and electrical impedance of the B81 was designed to replicate the B71. This was verified, as there was only a small deviation found at the mid frequencies of the frequency response where the B81 was 5.5 dB more efficient. Most importantly, it was found that the THD was considerably lower for the B81 up to 1000 Hz and

mainly unchanged at higher frequencies when driven by a constant voltage of 1 V_{RMS}. The maximum hearing levels, limited by a THD of 6% or an input voltage 6 V_{RMS} (whichever comes first), were found to be 10.7 to 22.0 dB higher for the B81 than for the B71 at frequencies below 1500 Hz and unchanged above. It was found that the B81 met the IEC 60645-1 (2012) requirements at all frequencies, while the B71 produced an output that was below the requirement at 250 Hz. When the THD for B71 is compensated for the actual hearing sensitivity of the harmonics, distortion at low frequencies is even worse and it is obvious that the improved performance offered by B81 is needed. To summarize:

- The Radioear B81 may offer a new era in low frequency bone conduction audiometry as it was found to generate less harmonic distortion and allow higher output levels than the B71 below 1500 Hz by using the BEST principle. It was also verified to be compatible with the same audiometers as it has an almost identical frequency response and electrical impedance as the B71. The B81 allows for routine bone conduction diagnostics to be performed also at 250 Hz, which has rarely been done before.

4.2 Vibrotactile Thresholds on the Mastoid and Forehead Position of Deaf Patients Using Radioear B71 and B81 (Paper II)

In this paper, the aim was to investigate the vibrotactile thresholds on the mastoid and forehead positions. A second objective was to compare the vibrotactile thresholds obtained from the two BC vibrators Radioear B71 and B81. In total 16 patients were measured, 31% were female and 69% male with average age 63 years. They were selected based on their audiogram data showing unmeasurable unaided hearing thresholds, thus diagnosed as bilateral deaf, to reduce the risk of responding to sound instead of vibrotactile sensation. All subjects were cochlear implant recipients, either uni- or bilaterally implanted, and their devices were switched off during the measurement.

It was found that the force level at which the vibrotactile thresholds were reached, increased with frequency from 125 up to 500 Hz, but remained constant for higher frequencies up to 2 kHz. There was no statistically significant difference in vibrotactile thresholds between the mastoid and forehead position in terms of force levels (dB re 1 μN), but, as expected, an average difference of 10 and 9 dB (B71 and B81, respectively) was found in terms of hearing levels. At 125 Hz, there was a statistically significant difference between the two devices and the vibrotactile thresholds measured with B71 were reached at a lower force level than with B81, both on the mastoid process (5 dB) and the forehead (7 dB) position. At the detected vibrotactile threshold levels, the B71 was found to generate higher THD than the B81, especially at the lowest measured frequency of 125 Hz, where B71

generated 31.6% THD and the B81 only 6.3%. To summarize:

- The vibrotactile thresholds measured on deaf patients using Radioear B71 and B81 were mainly reached at lower hearing levels at low frequencies, and distortion was believed to affect the value at 125 Hz when using B71. No statistically significant difference was found between the devices at higher frequencies, nor between the forehead and mastoid position.

4.3 Robustness and Lifetime of Active Transcutaneous Bone Conduction Devices (Paper III)

The aim of this study was to develop a set of methods for evaluating the mechanical robustness and estimating the lifetime of the implantable part of active transcutaneous bone conduction devices (BCDs), and to apply these methods on the bone conduction implant (BCI), developed at Chalmers University of Technology in collaboration with Sahlgrenska University Hospital in Göteborg. A secondary aim was to suggest relevant acceptance limits for the implant performance in the different tests. The robustness of the implant was determined through existing test procedures developed for cochlear implants, comprising a random vibration test, a shock test, a pendulum test and an impact test. Also, magnetically induced torque and demagnetization during magnetic resonance imaging (MRI) at 1.5 Tesla were investigated using a dipole electromagnet. Furthermore, a long-term age accelerated test was developed and used in order to estimate the expected lifetime of the implant.

The maximum limit for acceptance in the manufacturing based on the frequency response is set to $\pm$ 20% of the nominal value for the resonance frequency peaks and a 5 dB loss in the magnitude at the mid frequencies (2 kHz). In a sense, it will be reasonable to have the same criteria for mechanical robustness testing as for the maximum acceptance criteria in the manufacturing process for a particular device.

It was found that the mechanical shock and vibration test had no evident effect on the electro-acoustic performance. However, the tests are still relevant because they are based on realistic levels of normal sound exposure to active transcutaneous BCDs throughout their lifetime. No effect was observed on the electro-acoustic performance after the long-term age accelerated test (so far). The pendulum and impact tests simulate more dramatic and rare scenarios, such as those from accidents that cause external exposure or if the implant is roughly handled before or during surgery. It was found that those tests were the only mechanical tests that affected the electro-acoustic performance even if the change was within the maximum allowed limit and minor in terms of acceptable production variability.

Moreover, after the pendulum test, the lower and higher resonance peaks were shifted down in frequency with 13 and 9%, and with a maximum loss in magnitude of 1.1 and 4.1 dB, respectively. The impact test further shifted the higher resonance peak down with 8%, but otherwise, the performance was mainly unchanged. In the MRI testing at 1.5 Tesla, it was found that the transducer withstood the static magnetic field, and the magnetically induced torque on the transducer followed the shape of a sine curve with an amplitude of 0.135 Nm. To summarize:

- The Mechanical Robustness of active transcutaneous BCDs can be properly tested using a random vibration test, a shock test, a pendulum test and an impact test, and the lifetime can be estimated using a long-term age accelerated sound exposure test. By applying these tests to the BCI, the robustness was verified and the lifetime was estimated to be over 10 years for patients who are using their device for 10 hours on a daily basis. Also, the electromechanical robustness was verified using an MRI test at 1.5 Tesla. In order for the implant to pass the tests, resonance peaks should not change more than ±20% in frequency and the magnitude should not deteriorate more than 5 dB for the mid frequencies, typically measured at 2 kHz.

4.4 MRI Induced Torque and Demagnetization in Retention Magnets for a Bone Conduction Implant (Paper IV)

Paper IV comprises an investigation of the torque and demagnetization effects on the retention magnet used in the BCI during MRI. The aim of the study was to investigate these effects, both by experimental measurements using an electromagnet and by computer simulations using the software COMSOL Multiphysics 4.2 (COMSOL AB, Stockholm, Sweden).

The electromagnet was able to generate a uniform magnetic field of 1.5 Tesla, similar to the field in a 1.5 Tesla MRI scanner. The stray-field around the electromagnet was considerably lower than in a MRI scanner because a dipole magnet with a closed magnetic circuit was used. Therefore, this setup made the measurements easier as the electronic equipment could be used closer to the fairly strong, but uniform magnetic field. The retention magnets in the BCI is a pair of two permanent magnets, one positioned internally in the implanted part, and one positioned in the externally worn audio processor (AP). When evaluating the safety aspects of the BCI during MRI, only the internal permanent magnet needs to be considered, since the patient can easily remove the AP before entering the MRI environment. In order to investigate how coercivity affects demagnetization and torque, two types of permanent magnets with the same size and magnetization,

but different coercive field strengths were tested. Eight magnets had a higher coercivity than 2.5 Tesla (the standard BCI magnet) and four had lower coercivity (0.62-0.9 Tesla). Demagnetization was calculated as the percentage loss in retention force against a reference magnet before and after exposure to the magnetic field.

In the experiments, demagnetization (percentage loss in retention force) and maximum torque for the high coercive field magnets were in average found to be 7.7 ± 2.5 % and 0.20 ± 0.01 Nm, respectively; and 71.4 ± 19.1 % and 0.18 ± 0.01 Nm for the low coercive field magnets, respectively. The simulated maximum torque was found to be 0.34 Nm, which is 0.14 Nm higher than the measured torque in terms of amplitude. Initially, this deviation was assumed to mainly relate to an insufficient magnet model that did not include demagnetization characteristics, but was later found to be due to wrong disc radius being used in the calculations, as it was 12 mm, not 6 mm (used in Paper IV). By using the correct disc radius, the maximum torque is also doubled, and instead it becomes 0.40 ± 0.01 Nm and 0.36 ± 0.01 Nm for the high and low coercive field magnets, respectively. After this correction, there is still a difference between the simulated and measured maximum torque, but it is significantly reduced. To summarize:

- It was found that 1.5 Tesla MRI will only have a minor effect on the magnetization of the retention magnet in the BCI implant and it will still be able to retain the AP with a sufficient retention force. Caution should be taken to how the magnetically induced torque is handled by the attachment of the implant to the skull and a compression band might be used around the head to prevent movement of the implant caused by the magnet.

4.5 Magnetic Resonance Imaging Investigation of the Bone Conduction Implant - a pilot study at 1.5 Tesla (Paper V)

In Paper V, the aim was to investigate if the present design of the full BCI withstands MRI at 1.5 Tesla. In particular, by comparing maximum power output (MPO), THD and retention force before and after MRI as well as to evaluate the image artifact when the implant is attached over the skin on a test person's head. In this study, the transducer of the BCI was pressed against the skin on a test person similar to how a conventional bone conduction device on a softband transmits the vibrations from the transducer through the skin into the skull bone. This procedure made it possible for the test person to listen via the implant to find out if any sound is induced by the magnetic fields generated by the MRI scanner and also to verify the implant function between the tests by driving it with an AP.

Thus, one BCI implant was placed over the skin on a test person at the assumed location for implantation and then scanned in a 1.5 Tesla MRI scanner. Images were attained both with and without the implant, and in three orthogonal planes, for spin-echo (SE) and gradient-echo (GE) pulse sequences.

It was found that the exposure of 1.5 Tesla had only a minor effect on the MPO (decreased with an average of 1.1 $\pm$ 2.1 dB) and the THD remained unchanged above 300 Hz. Only a minor loss in retention force (5%) was found and the test person did neither hear any MRI induced sound nor felt any movement of the implant. The maximum size of the image artifact was measured as the maximum distance from the implant in the sagittal, coronal and axial plane and found to be 9, 10 and 9 cm for the GE pulse sequence and 8, 9 and 8 cm for the SE pulse sequence, respectively. It is clear from this study that image artifacts distort the image in the close vicinity of the implant and eliminates the possibility to visualize tissue properties in this region. The remaining parts of the brain image as well as images in the rest of the body are unaffected.

In the implanted unit of the BCI, the retention magnet is connected to the transducer casing with a relatively stiff titanium bar and the transducer casing is further rigidly attached with a titanium wire to the bone. This is assumed to prevent the magnet from moving and a compression band around the head might not be needed, even if it is recommended for extra caution. To summarize:

- The study indicated that no induced BC sound can be heard from the implant during MRI at 1.5 Tesla, and the effects on the implants' output force, distortion and retention force were minor, but the image was distorted in the vicinity of the implant to a maximum distance of 10 cm. Most importantly, it was concluded based on the minor performance effects that the current BCI design may pass an approval to be MR conditional up to 1.5 Tesla.

4.6 The Bone Conduction Implant - Clinical results of the first six patients (Paper VI)

The aim of this study was to investigate the patients' audiological and quality of life outcomes by comparing the six month follow-up data of the first six BCI patients with the unaided condition and with a BAHA (Ponto Pro Power, Oticon Medical, Askim, Sweden) on a softband. The BCI offers a direct and osseointegrated bone drive, while the BAHA on softband is placed externally on the head with the skin in-between the transducer and bone.

The patients' audibility was tested using warble tones, speech recognition in quiet and in noise, and the patients' quality of life was evaluated using abbreviated profile of hearing aid benefit (APHAB) and Glasgow benefit inventory (GBI) questionnaires.

A statistically significant improvement (α=0.05) with the BCI over the un-

aided condition was found in all audiometric tests and questionnaires. The average improvement was found to be 31.0 dB in hearing thresholds, 27.0 dB in speech recognition threshold in quiet and 51.2% in speech recognition score in noise. The signal to noise ratio at speech level for the BCI was found to be -5.5 dB. Audiometric results as well as the subjective measures of quality of life were similar or better with the BCI as compared with BAHA on softband. To summarize:

- The clinical study of the first six BCI patients showed a significant improvement with the BCI over the unaided condition and, in comparison with BAHA on softband (skin drive), the BCI provides either similar or better rehabilitation for patients with conductive or mild-to-moderate mixed hearing loss. Also, it was found that the surgery is straightforward, uncomplicated and safe for the patients.

Chapter 5

Summary of thesis and future work

5.1 Summary of thesis

Over the years, the variety of devices and new technologies has increased in the field of bone conduction hearing and today there is a wide range of possibilities offered when it comes to both audiometry and rehabilitation of conductive hearing losses. In the transition from conventional devices, the trend is towards audiometric devices with improved low frequency performance and hearing implants with transcutaneous solutions that keep the skin intact. In this thesis, the main conclusions are:

- The Radioear B81 may offer a new era in low frequency bone conduction audiometry as it was found to generate less harmonic distortion and allow higher output levels than the B71 below 1500 Hz by using the BEST principle.
- The THD generated by B71 was found to affect the vibrotactile threholds at 125 Hz.
- The BCI implant has been verified as mechanically robust and its lifetime is estimated to be over 10 years for patients using their device for 10 hours on a daily basis.
- The current BCI design should pass an approval to be MR conditional up to 1.5 Tesla.
- The BCI is a viable rehabilitation alternative for patients with conductive or mild-to-moderate mixed hearing loss.

5.2 Future work

5.2.1 The bone conduction implant

The current technical design of the BCI system is used in the implants of the first 16 patients in an ongoing clinical study. The aim of the clinical study is to gather evidence for CE-mark as a next step for becoming commercially available and FDA approved to be used in the United States. This might require minor design changes in order to comply with different standard requirements and for an efficient serial production to be possible. Some of those requirements, thoroughly investigated in Paper III, are for the implant to withstand mechanical stress from rough handling after manufacturing, during packaging, transportation and surgery, and to determine the expected lifetime for the implant in ordinary use. The implant should also withstand occasional mechanical stress that it might be exposed to during its lifetime when implanted in patients, including MRI scanning.

This first BCI implant design was found to withstand all tests and the lifetime was estimated to more than 10 years for patients who are wearing it for 10 hours on a daily basis. That estimation can possibly be verified in the future when the first BCI patients have worn their devices for 10 years or more. So far, audiometric measurements and patient related outcomes are stable, including the first patient who received the BCI implant four and a half years ago. In the future, the mechanical robustness and estimated lifetime will be investigated for a larger group of implants to draw more definite conclusions about the results. For that study, a method for performing several long-term tests in parallel might be developed, both in terms of how to expose several implants simultaneously and how to perform verification measurements of those implants. To increase the accuracy of the lifetime estimation even more, an investigation of the average BCI usage time among the operated patients might be performed.

The results in the clinical study (Paper V) are based on the 6-month follow-up data from the first six BCI patients. Today, longer follow-up time (up to three years) as well as data from more patients has contributed to more definite results that will be published in a scientific journal.

Regarding the safety when performing MRI of patients who are using the BCI implant, which was studied in Paper III, IV and V, more implants and test subjects, as well as different pulse sequences, should be tested in the future. It is also common to use MRI scanners with higher static magnetic field strengths, such as 3 Tesla, which should be investigated as well. So far, electromagnetically induced heat has not been prioritized to investigate since this effect has shown no effect on similar hearing implants in other studies. In fact, hearing implants are relatively small in relation to the wavelength of the RF-fields, and the risk is higher for larger implants with long electrically conductive materials, such as pacemaker leads. However, the risk for MRI induced heat in hearing implants might increase in the future if it becomes more common to use MRI scanners with higher magnetic field strengths, which shortens the wavelength of the RF-fields. Regarding patients

who regularly need to perform MRI, also the effects of repetitive exposure have to be considered. For comparison reasons of the torque experiments in Paper IV, the study included a simulation part where the maximum induced torque (0.34 Nm) was compared with the experiments (0.40 Nm). The difference is assumed to relate to an insufficient model of the retention magnet in the simulation program that does not include demagnetization characteristics. In the future, a more extensive simulation model of the retention magnet is recommended, also for studies at fields higher than 1.5 Tesla where experimental measurements are more difficult to perform. The focus in future MRI related studies will be to further investigate the requirements for passing approval at 1.5 and 3 Tesla MRI, both by simulation and experiments.

5.2.2 Bone conduction vibrators

As the Radioear B81 offers a better low frequency performance than B71, it might be beneficial for other applications as well, such as auditory brainstem response (ABR) and vestibular evoked myogenic potential (VEMP). In future studies of the Radioear B81, its application as a BC vibrator for VEMP and ABR will be thoroughly investigated, since the B71 was not optimal due to its low output and high distortion at low frequencies. The electromagnetic interference with ABR electrodes is also one of the reasons why it is difficult to measure ABR using the B71. Various methods for reducing this effect will be investigated, e.g. by using a B81 which has another type of soft iron loop for the dynamic flux that is believed to cause a lower stray-field around the transducer.

Dizziness is a very common anxiety-provoking symptom that can be caused by many different diseases, such as Ménières disease, multiple sclerosis and many more (Pollak et al., 2003; Zhou and Cox, 2004). For about 50% of all patients, the symptom is linked to a disease in the balance organ (Geisler, 2016). In Sweden, every third woman and every seventh man in the age 20-65 years old are suffering from dizziness or vertigo disorders and the number increases to almost 50% at older age for both men and women (Mendel, 2007). There are also other diseases linked to the symptom of dizziness that are related to blood circulation, stroke and tumors, but also to diseases that affects the nerve functions in the brain. It is therefore very important to be able to make an as correct as possible diagnosis of patients with balance organ disorders (Geisler, 2016).

Some decades ago, it was discovered that the function of the balance organ (especially the otolitic organ containing Saccule and Utricule) and its connection to the brain could be diagnosed measuring VEMP (Zhou and Cox, 2004). When the vestibularis part of the balance organ is mechanically stimulated, it involuntarily as a reflex transmits an impulse signal through the balance nerve via the brain to contract the cervical muscles of the neck or causing eye movements. These muscle contractions measured on the neck is called cVEMP (cervical) or on the eye oVEMP (ocular) (Curthoys, 2010).

The first way to mechanically stimulate the vestibularis organ was by inducing a controlled mechanical impulse from a specially designed hammer. However, it was difficult to control the force with the hammer, and since the myogenic signal is weak, many impulses are required to obtain an averaged response signal. A later employed method is to place a speaker in the ear canal and by a low frequent sound at a relatively high level mechanically excite the vestubularis organ, and this is the prevalent way of evoking VEMP today. To mechanically stimulate the vestibular organ in this way is feasible as the vestibular organ is located in the cochlear fluid space. The reflex muscle response measured by the electrodes evoked by an AC sound is from now on called AC-VEMP. The disadvantage with this method is that an uncomfortably high sound (greater than 90-95 dB SPL) is required to reach the threshold of the reflex. To have a significant supra threshold response the sound levels should be rather greater than 100 dB SPL which is very high and may cause an, at least temporary, hearing loss. Therefore, it is also almost impossible to use AC-VEMP in patients who have a significant conduction hearing loss because of power limitation of the miniature speakers used in conventional equipment (Geisler, 2016).

A more appropriate method has recently been introduced to the field and is based on stimulating the vestibularis organ via induced low frequency bone conduction (BC) sound, generated by an audiometric BC vibrator (Zhou and Cox, 2004). The response is then consequently called BC-VEMP, which is very similar to AC-VEMP, but BC-VEMP is based on vibrations transmitted through the skull bone. Hence, the response is independent on the condition of the outer and middle ear i.e. is not negatively influenced by a conductive hearing loss. There is no transducer available on the market that is designed specifically for inducing these low frequency vibrations into the skull bone, and typically so far, the conventional audiometric BC vibrator Radioear B71 has been used. This and other BC vibrators are designed for hearing threshold measurements and thus having a higher resonance frequency than what seem to be optimal for the application of BC-VEMP. It has recently been shown that a higher BC-VEMP response is obtained at lower frequencies (optimum between 300 and 350 Hz), but where B71 is unable to generate sufficient output force with low distortion (Todd et al., 2000; Welgampola et al., 2003). Therefore, BC-VEMP has so far been performed at 500 Hz where the B71 has its main resonance frequency giving sufficient output force without producing too much harmonic distortion. Hence, the uncomfortably high excitation sound in AC-VEMP can be further reduced if the BC-VEMP is performed at a lower frequency. In a study by Fredén Jansson et al. (2015), it was found that B81 generates less distortion at higher hearing levels than B71 up to 1.5 kHz, with the maximum difference of 22 dB at 250 Hz. This strongly indicates that it is possible to develop a BC vibrator for low frequency BC-VEMP measurement, for example at 250 Hz, which will be the focus in a future study. That study will also include a clinical investigation by measuring BC-VEMP in patients with conductive hearing losses.

Appendices

Appendix A

Calibration of the artificial mastoid B&K 4930

When the electro-acoustic performance of a bone conduction (BC) vibrator is evaluated, measurement equipment with specific filter characteristics require calibration. Therefore, in the measurement setup used in Paper I, both the artificial mastoid B&K 4930 and the charge amplifier B&K 2635 (Brüel & Kjær Sound & Vibration Measurement A/S, Denmark) needed to be calibrated.

The output signal from the artificial mastoid is a voltage V_{out} that is generated when a force F_{in} is applied on the surface of the rubber pad, see Figure A.1. When F_{in} is a sinus signal with an amplitude of 1 N and a frequency of 1000 Hz, V_{out} should have an amplitude of 120 mV according to the calibration sheet of the artificial mastoid. This force to voltage relation is commonly referred to as the force sensitivity constant α and is equal to 120 mV/N. It specifies the sensitivity at 1 kHz and is sometimes used to determine the sensitivity for the total frequency range of the artificial mastoid between 100 and 10 000 Hz. This frequency dependence is commonly referred to as the pad correction curve $P(j\omega)$ (FigureA.2) and is defined as the ratio between $F_{in}(j\omega)$ and $V_{out}(j\omega)$ as follows

$$P(j\omega) = \frac{F_{in}(j\omega)}{V_{out}(j\omega)}. \tag{A.1}$$

The pad correction is then used to determine the frequency spectrum of $F_{in}(j\omega)$ of the BC vibrator, from which the total harmonic distortion (THD) and the frequency response $G(j\omega)$ can be calculated. The frequency response of the BC vibrator is given by the input voltage $V_{in}(j\omega)$ to $F_{in}(j\omega)$,

$$G(j\omega) = \frac{F_{in}(j\omega)}{V_{in}(j\omega)} = \frac{P(j\omega)V_{out}(j\omega)}{V_{in}(j\omega)}. \tag{A.2}$$

The pad correction curve was calculated from measurements using an impedance head B&K 8000 between a minishaker B&K 4810 and the artificial mastoid. There

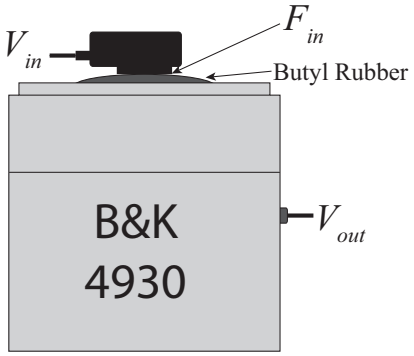

Figure A.1: Attachment of the bone conduction vibrator on the artificial mastoid. The input voltage to the bone vibrator is V_{in}, which applies a force F_{in} to the rubber pad so and generates an output voltage V_{out} from the artificial mastoid.

are two output signals from the impedance head, $A(j\omega)$ and $F(j\omega)$. First, the shape $P'(j\omega)$ of the pad correction curve has to be found and then it is scaled to intersect α=120 mV/N at 1000 Hz so that $P(j2\pi1000) = \alpha$ and

$$P(j\omega) = \alpha \frac{P'(j\omega)}{P'(j2\pi1000)}, \tag{A.3}$$

where

$$P'(j\omega) = \frac{F'_{in}(j\omega)}{V_{out}(j\omega)}. \tag{A.4}$$

The primed input force $F'_{in}(j\omega)$ has the shape of $F_{in}(j\omega)$ and should be scaled with a sensitivity constant to give the correct force. This constant is unknown because the sensitivity constants for the output signals from the impedance head are often uncalibrated. However, the ratio between $F(j\omega)$ and $A(j\omega)$, denoted K, can easily be found and is enough information for finding $P(j\omega)$ if at least α is known. In the time domain, velocity is the integrated acceleration, which corresponds to $A(j\omega)/j\omega$ in the frequency domain, and this ratio should be multiplied by the mechanical impedance $Z_m(j\omega)$ of the artificial mastoid to give the force

$$F_{in}(j\omega) = \frac{A(j\omega)}{j\omega} Z_m(j\omega). \tag{A.5}$$

The acceleration signal from the impedance head is the unscaled acceleration, denoted $A'(j\omega)$, and is measured as a voltage rather than an acceleration. This gives the measured and unscaled input force

$$F'_{in}(j\omega) = \frac{A'(j\omega)}{j\omega} Z_m(j\omega). \tag{A.6}$$

Inserting equation (A.6) in (A.4) then gives

$$P(j\omega)' = \frac{A'(j\omega)}{j\omega} \frac{Z_m(j\omega)}{V_{out}(j\omega)}. \tag{A.7}$$

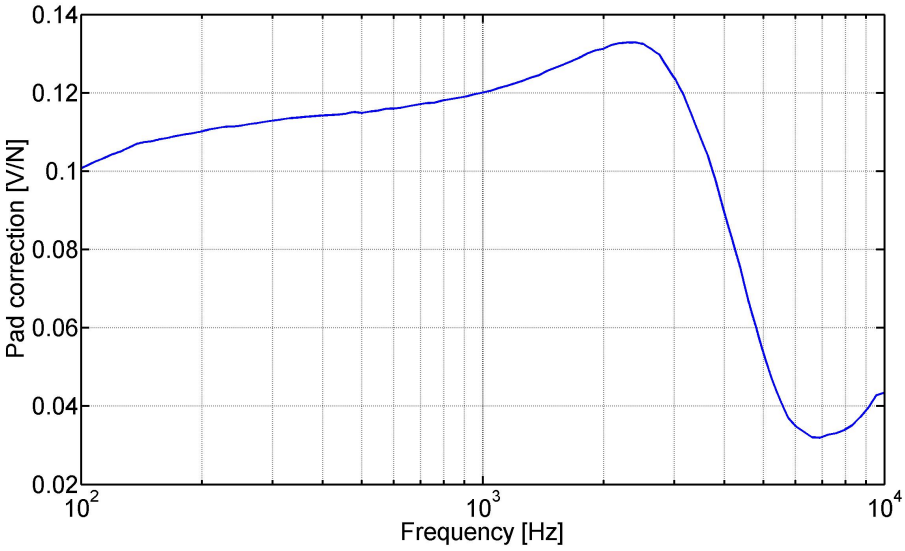

Figure A.2: The pad correction curve of the artificial mastoid B&K 4930

Inside the impedance head there is an inherently mass m_0=1.1 g below a force gauge, which has a mechanical impedance $Z_0(j\omega)$=$j\omega m_0$ that is mechanically coupled in series with $Z_m(j\omega)$. Therefore, $F(j\omega)$ acts on m_0 in series with the artificial mastoid, while $F_{in}(j\omega)$ is only the force on the rubber pad, which gives that

$$F(j\omega) = \frac{A(j\omega)}{j\omega}\left(Z_0(j\omega) + Z_m(j\omega)\right) = \frac{A(j\omega)}{j\omega}\left(j\omega m_0 + Z_m(j\omega)\right), \tag{A.8}$$

and the mechanical impedance of the artificial mastoid becomes

$$Z_m(j\omega) = j\omega\left(\frac{F(j\omega)}{A(j\omega)} - m_0\right), \tag{A.9}$$

see Figure A.3. The input force $F_{in}(j\omega)$ to the rubber pad should not be confused with the output force $F(j\omega)$ from the impedance head. Furthermore, the sensitivity constant for $F(j\omega)$ is uncalibrated and the voltage measured from the force gauge of the impedance head is an unscaled force, denoted $F'(j\omega)$. By using the ratio K, neither the acceleration nor the force sensitivity constants are needed, which gives

$$Z_m(j\omega) = j\omega\left(\frac{F'(j\omega)}{A'(j\omega)}K - m_0\right), \tag{A.10}$$

where K is a property of the impedance head that has to be determined in a separate measurement by connecting the impedance head to the minishaker and load it with a known mass m. This mass will be mechanically coupled in series

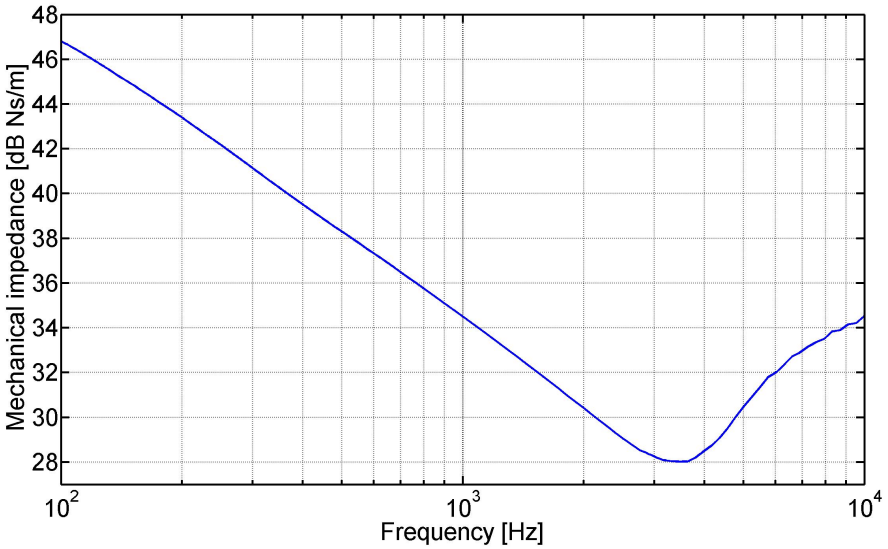

Figure A.3: The mechanical impedance of the artificial mastoid B&K 4930

with m_0 and the output force $F(j\omega)$ will act on those two masses so that

$$F(j\omega) = \frac{A(j\omega)}{j\omega}\left(j\omega m_0 + j\omega m\right), \tag{A.11}$$

which implies that the ratio between $F(j\omega)$ and $A(j\omega)$ will be the total mass so that

$$\frac{F(j\omega)}{A(j\omega)} = m_0 + m. \tag{A.12}$$

If the frequency response from the measured voltages $A'(j\omega)$ to $F'(j\omega)$ is not equal to the total mass, it should be corrected by K so that

$$\frac{F'(j\omega)}{A'(j\omega)}K = m_0 + m. \tag{A.13}$$

Then K can be calculated as

$$K = \frac{A'(j\omega)}{F'(j\omega)}\left(m_0 + m\right). \tag{A.14}$$

When K is to be determined, a relatively small mass should be used so that a flat frequency response is achieved at the lower frequencies and not influenced by the resonance peak.

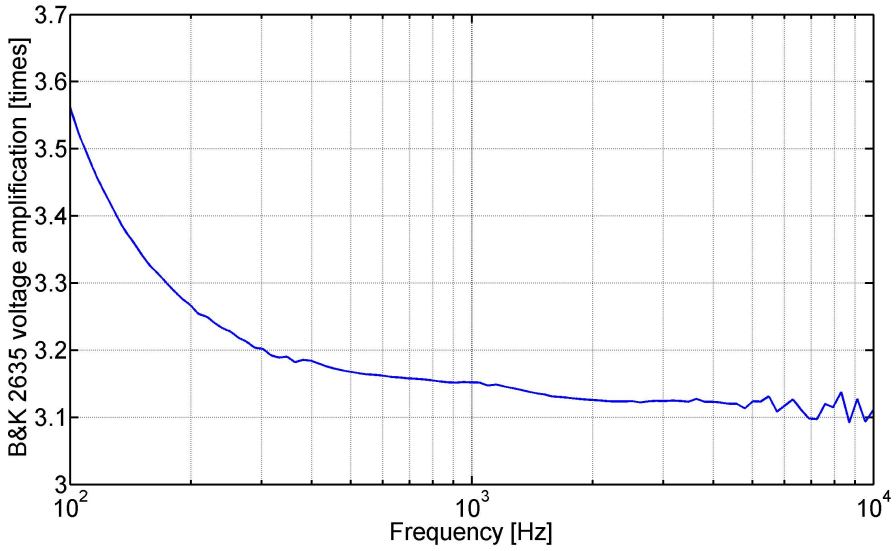

Figure A.4: The voltage amplification of the charge amplifier B&K 2635

To compensate for the filter characteristics $H(j\omega)$ of the charge amplifier (Figure A.4), the difference in frequency response of a bone vibrator measured with $(Y(j\omega))$ and without $(X(j\omega))$ the amplifier, was found to be

$$H(j\omega) = \frac{Y(j\omega)}{X(j\omega)}. \tag{A.15}$$

A summary of the calibration process of the artificial mastoid is given below:

- First, obtain K by adding a mass on top of the impedance head when it is attached to the minishaker and measure

$$K = \frac{A'(j\omega)}{F'(j\omega)} (m_0 + m) .$$

- Remove the added mass and attach the minishaker and impedance head upside down on the rubber pad of the artificial mastoid with 5.4 N. Obtain $Z_m(j\omega)$ by measuring

$$Z_m(j\omega) = j\omega \left(\frac{F'(j\omega)}{A'(j\omega)} K - m_0 \right) .$$

- Keep $Z_m(j\omega)$ (Figure A.3) and measure the unscaled pad correction curve $P'(j\omega)$ as

$$P(j\omega)' = \frac{A'(j\omega)}{j\omega} \frac{Z_m(j\omega)}{V_{out}(j\omega)}.$$

- Finally, scale the curve to intersect α=120 mV/N at 1 kHz.

$$P(j\omega) = \alpha \frac{P'(j\omega)}{P'(j2\pi 1000)}.$$

- The dynamic force acting on the rubber pad can now be found by measuring the output voltage $V_{out}(j\omega)$ and multiplying it with the pad correction curve, which gives

$$F_{in}(j\omega) = P(j\omega) V_{out}(j\omega).$$

- The frequency response $G(j\omega)$ of the bone vibrator that relates the input voltage $V_{in}(j\omega)$ to the input force $F_{in}(j\omega)$ can be found as

$$G(j\omega) = \frac{F_{in}(j\omega)}{V_{in}(j\omega)} = \frac{P(j\omega) V_{out}(j\omega)}{V_{in}(j\omega)}.$$

Appendix **B**

Disc magnet **B**-field equation

This appendix summarizes how the derivation of a uniformly magnetized circular cylinder, given in Cheng (1989), was applied to the retention magnet of the BCI implant to determine equation (1) in the part of Paper II where the magnetically induced torque at 1.5 Tesla was simulated.

An object with a magnetic dipole moment has a magnetization vector $\mathbf{M}$. The partial scalar magnetic potential from each volume element at radial distance R is

$$dV_m = \frac{\mathbf{M}\cdot\hat{\boldsymbol{R}}}{4\pi R^2}, \tag{B.1}$$

where $\hat{\boldsymbol{R}}$ is the radial unit vector. Integration over the magnetized object's volume V' gives the total magnetic potential V_m as

$$V_m = \frac{1}{4\pi}\int_{V'} \frac{\mathbf{M}\cdot\hat{\boldsymbol{R}}}{R^2} dv'. \tag{B.2}$$

In cartesian coordinates, the radial distance R from the primed source point (x', y', z') to the fixed field point (x, y, z) can be written as

$$R = \sqrt{(x-x')^2 + (y-y')^2 + (z-z')^2}, \tag{B.3}$$

and the gradient of $1/R$ with respect to the primed coordinates is

$$\nabla'\left(\frac{1}{R}\right) = \frac{\hat{\boldsymbol{R}}}{R^2}. \tag{B.4}$$

Then the following vector identity can be used

$$\nabla'\cdot\left(\frac{1}{R}\right)\mathbf{M} = \left(\frac{1}{R}\right)\nabla'\cdot\mathbf{M} + \mathbf{M}\cdot\nabla'\left(\frac{1}{R}\right). \tag{B.5}$$

Inserting equation (B.5) in (B.2) gives the following expression for the magnetic potential

$$V_m = \frac{1}{4\pi}\left[\int_{V'} \nabla' \cdot \left(\frac{\mathbf{M}}{R}\right) dv' - \int_{V'} \frac{\nabla' \cdot \mathbf{M}}{R} dv'\right]. \tag{B.6}$$

By applying the divergence theorem on the first integral in equation B.6, it can be written as a surface integral over the magnetized object's surface S' and the new expression becomes

$$V_m = \frac{1}{4\pi} \oint_{S'} \frac{\mathbf{M} \cdot \hat{\boldsymbol{n}}'}{R} ds' + \frac{1}{4\pi} \int_{V'} \frac{-(\nabla' \cdot \mathbf{M})}{R} dv', \tag{B.7}$$

where $\hat{\boldsymbol{n}}'$ is the normal vector to the surface of the magnetized object. Introducing equivalent charge densities $\rho_{ms} = \mathbf{M} \cdot \hat{\boldsymbol{n}}'$ and $\rho_m = -\nabla' \cdot \mathbf{M}$ gives

$$V_m = \oint_{S'} \frac{\rho_{ms}}{4\pi R} ds' + \int_{V'} \frac{\rho_m}{4\pi R} dv'. \tag{B.8}$$

For a cylindrical disc shaped magnet with the axial magnetization $\mathbf{M}=\hat{\boldsymbol{z}} M_0$ the charge densities becomes

$$\rho_{ms} = \begin{cases} M_0 & \text{on the top surface,} \\ -M_0 & \text{on the bottom surface,} \\ 0 & \text{on the side wall;} \end{cases}$$

$$\rho_m = 0 \qquad \text{in the interior.}$$

With surface charge densities located at the top and bottom of the magnet, the magnetic potential from the positive surface charges at distance R_+ is

$$V_{m+} = \frac{M_0 \pi b^2}{4\pi R_+}, \tag{B.9}$$

and for the negative surface charges at distance R_-

$$V_{m-} = -\frac{M_0 \pi b^2}{4\pi R_-}. \tag{B.10}$$

Then the total magnetic potential becomes

$$V_T = \frac{q_m}{4\pi}\left(\frac{1}{R_+} - \frac{1}{R_-}\right), \tag{B.11}$$

where $q_m = M_0 \pi b^2$. To simplify the expression in equation (B.11) and under the assumption that $R \gg b$, the distances R_+ and R_- can be approximated as

$$\frac{1}{R_+} \cong \left(R - \frac{L}{2}\cos\theta\right)^{-1} \cong R^{-1}\left(1 + \frac{L}{2R}\cos\theta\right) \tag{B.12}$$

and

$$\frac{1}{R_-} \cong \left(R + \frac{L}{2}\cos\theta\right)^{-1} \cong R^{-1}\left(1 - \frac{L}{2R}\cos\theta\right). \tag{B.13}$$

By inserting equations (B.12) and (B.13) in (B.11), the final expression for V_T will be

$$V_T \cong \frac{q_m L\cos\theta}{4\pi R^2} = \frac{\left(\pi b^2 M_0\right) L\cos\theta}{4\pi R^2} = \frac{M_T\cos\theta}{4\pi R^2}, \tag{B.14}$$

where $M_T = q_m L = M_0\pi b^2 L$ is the total dipole moment of the cylindrical magnet and the vectorized $\mathbf{B}$ field will thus be determined by

$$\mathbf{B} \cong -\mu_0\nabla V_T = \frac{\mu_0 M_T}{4\pi R^3}\left(\hat{\boldsymbol{R}}2\cos\theta + \hat{\boldsymbol{\theta}}\sin\theta\right), \tag{B.15}$$

which is equal to equation (1) in the simulation part of Paper II.

Appendix C

Simulations of the magnetically induced torque on a retention magnet during magnetic resonance imaging

The static magnetically induced torque on the retention magnet of the BCI implant was simulated in Paper IV using COMSOL Multiphysics 4.2 (COMSOL AB, Stockholm, Sweden) which is a software that can approximate solutions to electromagnetic problems using the finite element method. The retention magnet was modelled as a cylindrical disc with a remanent flux density of 1.08 Tesla in the axial direction and with a relative permeability of 1.05, both specified by the manufacturer. The inside of the MRI scanner was modelled as a sphere of air in a uniform background field of 1.5 Tesla. In experiments like these, the magnetic field representing the inside of the MRI scanner has in practice a fixed direction and the measureing object is rotated to measure the torque at different angles. In the simulation, the magnet was instead fixed and the direction of the background field rotated around the magnet in a parametric sweep from 0 to 180^o with steps of 10^o. The simulation resulted in a sine function in the interval of $0 \leq \alpha \leq 180^o$ with the maximum value of 0.337 Nm at 90^o (Figure C.1) and with a discretization error less than 0.6%.

The simulation domain was defined with respect to the magnetic flux density at the distance R from the permanent magnet which must be zero at the periphery of the sphere in order to include the total field in the numerical calculation. The mathematical expression for the flux density around a cylindrical disc shaped permanent magnet (Appendix B) is given by

$$\mathbf{B} \cong \frac{\mu_0 M_T}{4\pi R^3} \left(\hat{\boldsymbol{R}} 2\cos\theta + \hat{\boldsymbol{\theta}} \sin\theta \right), \tag{C.1}$$

and comprises one radial and one angular component expressed by the unit vectors $\hat{\boldsymbol{R}}$ and $\hat{\boldsymbol{\theta}}$, repectively.

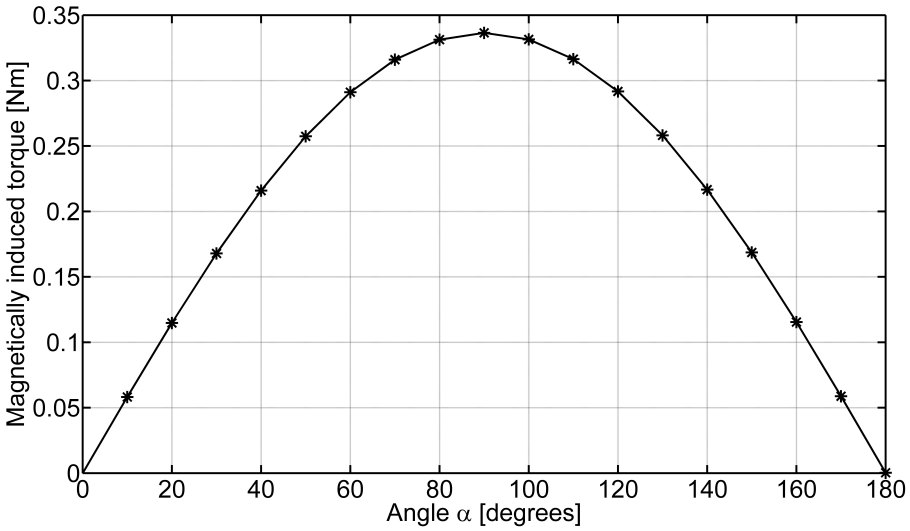

Figure C.1: Simulated static magnetic induced torque on the retention magnet of the BCI implant. A static uniform magnetic field of 1.5 Tesla was applied for angles between 0 and 180^o.

The magnetization M_T of the magnet is given in A/m and the angular position θ in radians. The zero boundary condition, which is fulfilled when the radius of the sphere is large enough, implies that the radial component becomes zero when $R = R_{sphere}$ so that

$$\mathbf{B}(R_{sphere}) \cong \hat{\boldsymbol{R}} \frac{2\mu_0 M_T \cos\theta}{4\pi R_{sphere}^3} = 0. \tag{C.2}$$

In order to find the optimal value of Rsphere, it was swept from 5 cm to 15 cm with a step of 1 cm and the maximum torque was found to have a maximum variation less than 0.01% between 7 and 15 cm. This variation is small compared to the discretization error (0.6%) and there is no need to make R_{sphere} bigger than 7 cm.

The mesh resolution was required to be higher close to the magnet where the field lines changes more rapidly than at the boundary of the sphere where the mesh can be coarser. Furthermore, both the maximum and minimum element size was refined until the discretization error was less than 1%. In addition, an extrapolation to zero cell size was performed using values from numerical computations where the minimum cell size was decreased from 2.8 to 0.25 μm, which resulted in a torque of 0.3385 Nm, see Figure C.2. Finally, with a discretization error less than 1%, the significant simulated torque was 0.34 Nm which is the simulation result presented in Paper II.

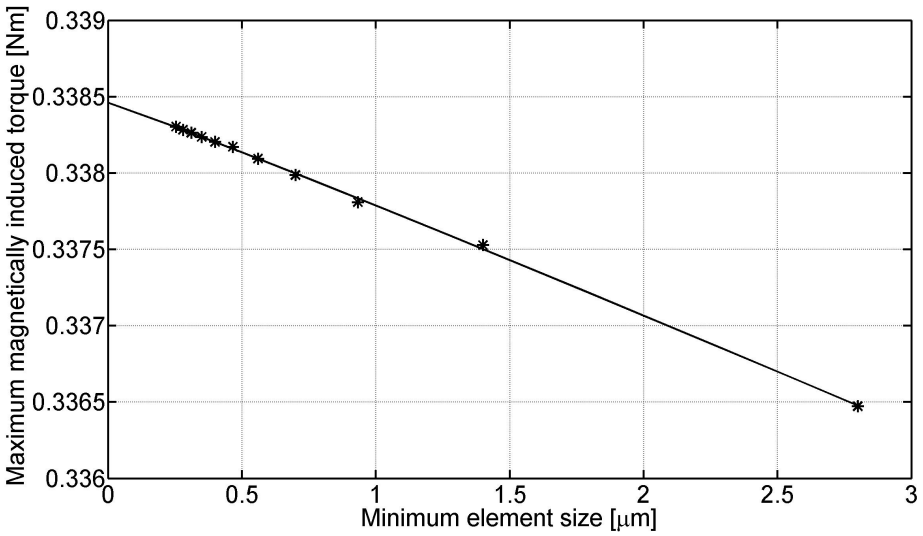

Figure C.2: The extrapolated curve (solid line) of the expected simulated magnetically induced torque when the cell size goes to zero. The simulated maximum magnetically induced torque ($*$) was swept for 10 exponentially distributed values of the minimum element size of the mesh.

Bibliography

Békésy, G. V. (1932). Zur theorie des hörens bei der schallaufnahme durch knochenleitung. *Annalen der Physik*, 405:111–136.

Beltrame, A. M., Martini, A., Prosser, S., Giarbini, N., and Streitberger, C. (2009). Coupling the vibrant soundbridge to cochlea round window: auditory results in patients with mixed hearing loss. *Otology & Neurotology*, 30(2):194–201.

Bushong, S. C. (2003). *Magnetic resonance imaging: physical and biological principles, 3rd edition*. Elsevier Health Sciences.

Cheng, D. K. (1989). *Field and wave electromagnetics*, volume 2. Addison-wesley New York.

Clark, J. G. (1981). Uses and abuses of hearing loss classification. *Asha*, 23(7):493–500.

Coey, J. M. (2010). *Magnetism and magnetic materials*. Cambridge University Press.

Curthoys, I. S. (2010). A critical review of the neurophysiological evidence underlying clinical vestibular testing using sound, vibration and galvanic stimuli. *Clinical Neurophysiology*, 121(2):132–144.

de Wolf, M. J., Hol, M. K., Huygen, P. L., Mylanus, E. A., and Cremers, W. (2008). Nijmegen results with application of a bone-anchored hearing aid in children: simplified surgical technique. *Annals of Otology, Rhinology & Laryngology*, 117(11):805–814.

Dun, C. A., Faber, H. T., de Wolf, M. J., Mylanus, E. A., Cremers, C. W., and Hol, M. K. (2012). Assessment of more than 1,000 implanted percutaneous bone conduction devices: skin reactions and implant survival. *Otology & Neurotology*, 33(2):192–198.

Eeg-Olofsson, M., Håkansson, B., Reinfeldt, S., Taghavi, H., Lund, H., Fredén Jansson, K.-J. F., Håkansson, E., and Stalfors, J. (2014). The bone conduction implantâfirst implantation, surgical and audiologic aspects. *Otology & Neurotology*, 35(4):679–685.

Fredén Jansson, K.-J., Håkansson, B., Johannsen, L., and Tengstrand, T. (2015). Electro-acoustic performance of the new bone vibrator radioear b81: A comparison with the conventional radioear b71. *International journal of audiology*, 54(5):334–340.

Gallichan, M.-C., Ravenna, S., Giguere, C., Leroux, T., Wu, L., and Wong, G. S. (1998). High-frequency bone conduction audiometry using a piezoelectric transducer. *Canadian Acoustics*, 26(3):70–71.

Geisler, C. (2016). Orsaker till yrsel. `http://yrselcenter.se/orsaker-till-yrsel/`. [Online; accessed March 2016].

Haacke, E. M., Brown, R. W., Thompson, M. R., and Venkatesan, R. (1999). *Magnetic resonance imaging: physical principles and sequence design*. John Wiley & Sons.

Håkansson, B. (2011). The future of bone conduction hearing devices. In *Implantable Bone Conduction Hearing Aids*, volume 71, pages 140–152. Karger Publishers.

Håkansson, B., Reinfeldt, S., Eeg-Olofsson, M., Östli, P., Taghavi, H., Adler, J., Gabrielsson, J., Stenfelt, S., and Granström, G. (2010). A novel bone conduction implant (bci): engineering aspects and pre-clinical studies. *International journal of audiology*, 49(3):203–215.

Håkansson, B., Tjellström, A., and Rosenhall, U. (1984). Hearing thresholds with direct bone conduction versus conventional bone conduction. *Scand. Audiol.*, 13:3–13.

Håkansson, B., Tjellström, A., Rosenhall, U., and Carlsson, P. (1985). The bone-anchored hearing aid: principal design and a psychoacoustical evaluation. *Acta oto-laryngologica*, 100(3-4):229–239.

Håkansson, B. E. (2003). The balanced electromagnetic separation transducer: A new bone conduction transducer. *The Journal of the Acoustical Society of America*, 113(2):818–825.

Hultcrantz, M. and Lanis, A. (2014). A five-year follow-up on the osseointegration of bone-anchored hearing device implantation without tissue reduction. *Otology & Neurotology*, 35(8):1480–1485.

ISO 389-3 (1994). *Acoustics - Reference zero for the calibration of audiometric equipment. Part 3: Reference equivalent threshold force levels for pure tones and bone vibrators.* Geneva: ISO; 1994-10-01.

Jesacher, M. O., Kiefer, J., Zierhofer, C., and Fauser, C. (2010). Torque measurements of the ossicular chain: implication on the mri safety of the hearing implant vibrant soundbridge. *Otology & Neurotology*, 31(4):676–680.

Kiringoda, R. and Lustig, L. R. (2013). A meta-analysis of the complications associated with osseointegrated hearing aids. *Otology & Neurotology*, 34(5):790–794.

Lidén, G., Jacobsson, M., Håkansson, B., Tjellström, A., Carlsson, P., Ringdahl, A., and Erlandson, B.-E. (1990). Ten years of experience with the swedish bone-anchored hearing system. *Annals of Otology, Rhinology & Laryngology*, 99(10_suppl):1–16.

McComb, C., Allan, D., and Condon, B. (2009). Evaluation of the translational and rotational forces acting on a highly ferromagnetic orthopedic spinal implant in magnetic resonance imaging. *Journal of Magnetic Resonance Imaging*, 29(2):449–453.

MED-EL (2014). Vibrant soundbridge system. `http://s3.medel.com.s3.amazonaws.com/pdf/28477_10_Factsheet%20VSB%20System%20%28english%29-8seitig_screen6.pdf`. [Online; accessed 20-Dec-2014].

Mendel, B. (2007). *Yrsel ur patientens perspektiv: En klinisk och epidemiologisk studie på personer med öronrelaterad yrsel.* Institutionen för neurobiologi, vårdvetenskap och samhälle/Department of Neurobiology, Care Sciences and Society.

Nyenhuis, J. A., Park, S.-M., Kamondetdacha, R., Amjad, A., Shellock, F. G., and Rezai, A. R. (2005). Mri and implanted medical devices: basic interactions with an emphasis on heating. *Device and Materials Reliability, IEEE Transactions on*, 5(3):467–480.

Pollak, L., Klein, C., Rafael, S., Vera, K., and Rabey, J. M. (2003). Anxiety in the first attack of vertigo. *Otolaryngology–Head and Neck Surgery*, 128(6):829–834.

Radioear (2015a). B71W Bone transducers. `http://radioear.us/pdfs/RE_B71W_LR.pdf`. [Online; accessed 16-Feb-2015].

Radioear (2015b). B72 Bone Transducers. `http://radioear.us/bone-transducers.html`. [Online; accessed 16-Feb-2015].

Radioear (2015c). Over 100 years of innovation and evolution with a constant focus on the needs of the audiology community. `http://www.radioear.us/about.html`. [Online; accessed 07-March-2017].

Reinfeldt, S., Håkansson, B., Taghavi, H., and Eeg-Olofsson, M. (2015a). New developments in bone-conduction hearing implants: a review. *Medical devices (Auckl, NZ)*, 16(8):79–93.

Reinfeldt, S., Håkansson, B., Taghavi, H., Fredén Jansson, K.-J., and Eeg-Olofsson, M. (2015b). The bone conduction implant: Clinical results of the first six patients. *International journal of audiology*, 54(6):408–416.

Richards, W. D. and Frank, T. (1982). Frequency response and output variations of radioear b-71 and b-72 bone vibrators. *Ear and hearing*, 3(1):37–38.

Shellock, F. G. (2012). *Reference manual for magnetic resonance safety, implants and devices*. Biomedical research publishing group.

Shellock, F. G., Kanal, E., and Gilk, T. B. (2011). Regarding the value reported for the term âspatial gradient magnetic fieldâ and how this information is applied to labeling of medical implants and devices. *American Journal of Roentgenology*, 196(1):142–145.

Snik, A. F., Mylanus, E., Proops, D. W., Wolfaardt, J. F., Hodgetts, W. E., Somers, T., Niparko, J. K., Wazen, J. J., Sterkers, O., Cremers, C., et al. (2005). Consensus statements on the baha system: where do we stand at present? *The Annals of otology, rhinology & laryngology. Supplement*, 195:2–12.

Stenfelt, S. and Goode, R. L. (2005). Bone-conducted sound: Physiological and clinical aspects. *Otology Neurotology*, 26:1245–1261.

Taghavi, H., Håkansson, B., Reinfeldt, S., Eeg-Olofsson, M., and Akhshijan, S. (2012). Feedback analysis in percutaneous bone-conduction device and bone-conduction implant on a dry cranium. *Otology & Neurotology*, 33(3):413–420.

Taghavi, H., Håkansson, B., Reinfeldt, S., Eeg-Olofsson, M., Jansson, K.-J. F., Håkansson, E., and Nasri, B. (2015). Technical design of a new bone conduction implant (bci) system. *International journal of audiology*, 54(10):736–744.

Teissl, C., Kremser, C., Hochmair, E. S., and Hochmair-Desoyer, I. J. (1998). Cochlear implants: in vitro investigation of electromagnetic interference at mr imaging–compatibility and safety aspects. *Radiology*, 208(3):700–708.

Tjellström, A., Håkansson, B., and Granström, G. (2001). Bone-anchored hearing aids: current status in adults and children. *Otolaryngologic Clinics of North America*, 34(2):337–364.

Todd, N. P. M., Cody, F. W., and Banks, J. R. (2000). A saccular origin of frequency tuning in myogenic vestibular evoked potentials?: implications for human responses to loud sounds. *Hearing research*, 141(1):180–188.

Todt, I., Wagner, J., Goetze, R., Scholz, S., Seidl, R., and Ernst, A. (2011). Mri scanning in patients implanted with a vibrant soundbridge. *The Laryngoscope*, 121(7):1532–1535.

Welgampola, M., Rosengren, S., Halmagyi, G., and Colebatch, J. (2003). Vestibular activation by bone conducted sound. *Journal of Neurology, Neurosurgery & Psychiatry*, 74(6):771–778.

Zhou, G. and Cox, L. C. (2004). Vestibular evoked myogenic potentialshistory and overview. *American Journal of Audiology*, 13(2):135–143.

Part II

Appended papers